BI-TP 2016/05

Free Energy of a Heavy Quark–Antiquark Pair in a Thermal Medium from AdS/CFT

arXiv:1605.07181v1 [hep-th] 23 May 2016

Carlo Ewerz,[a,b,c] **Olaf Kaczmarek,**[d] **Andreas Samberg**[a,b]

[a] *Institut für Theoretische Physik, Ruprecht-Karls-Universität Heidelberg, Philosophenweg 16, D-69120 Heidelberg, Germany*

[b] *ExtreMe Matter Institute EMMI, GSI Helmholtzzentrum für Schwerionenforschung, Planckstraße 1, D-64291 Darmstadt, Germany*

[c] *Frankfurt Institute for Advanced Studies, Ruth-Moufang-Straße 1, D-60438 Frankfurt, Germany*

[d] *Fakultät für Physik, Universität Bielefeld, D-33615 Bielefeld, Germany*

E-mail: c.ewerz@thphys.uni-heidelberg.de, okacz@physik.uni-bielefeld.de, a.samberg@thphys.uni-heidelberg.de

Abstract: We study the free energy of a heavy quark–antiquark pair in a thermal medium using the AdS/CFT correspondence. We point out that a commonly used prescription for calculating this quantity leads to a temperature dependence in conflict with general properties of the free energy. The problem originates from a particular way of subtracting divergences. We argue that the commonly used prescription gives rise to the binding energy rather than the free energy. We consider a different subtraction procedure and show that the resulting free energy is well-behaved and in qualitative agreement with results from lattice QCD. The free energy and the binding energy of the quark pair are computed for $\mathcal{N} = 4$ supersymmetric Yang–Mills theory and several non-conformal theories. We also calculate the entropy and the internal energy of the pair in these theories. Using the consistent subtraction, we further study the free energy, entropy, and internal energy of a single heavy quark in the thermal medium for various theories. Also here the results are found to be in qualitative agreement with lattice QCD results.

Contents

1 Introduction 1

2 String in general AdS-type metric 4

3 Free energy versus binding energy of a heavy quark pair 8

4 Free energy and binding energy in $\mathcal{N} = 4$ supersymmetric Yang–Mills theory 12

5 Free energy and binding energy in non-conformal models 16

6 Entropy and internal energy of a heavy quark pair 22

7 Free energy, entropy, and internal energy of a single heavy quark 26

8 Summary and conclusions 33

A Computation of the entropy of a heavy quark pair 34

1 Introduction

The AdS/CFT correspondence [1–3] has become a valuable method for studying strongly coupled gauge theories. In its original form, the correspondence asserts that string theory of type IIB on an anti-de Sitter space, $\mathrm{AdS}_5 \times S_5$, provides an equivalent description of a particular conformal field theory, namely $\mathcal{N} = 4$ supersymmetric $SU(N_\mathrm{c})$ Yang–Mills theory (SYM) in four spacetime dimensions. This holographic duality is particularly useful in the limit of large N_c and large 't Hooft coupling $\lambda = g^2_\mathrm{YM} N_\mathrm{c}$ in the gauge theory, as then the dual description reduces to (super)gravity on $\mathrm{AdS}_5 \times S_5$. Remarkably, the weak-coupling limit of the gravity side corresponds to the strong-coupling limit of the gauge theory side. A finite temperature T of the gauge theory corresponds to a black brane with Hawking temperature T in the AdS_5 space. AdS/CFT hence offers an intrinsically nonperturbative framework that allows one to study strongly coupled gauge theories both at vanishing and at finite temperature. The original AdS/CFT correspondence has been extended in various ways and by now has found applications to strongly coupled systems in many areas of physics. One of the most promising applications of the AdS/CFT correspondence (or more generally gauge/gravity correspondence) concerns the physics of hot, strongly coupled gauge theory plasmas, see for example [4, 5] for recent reviews. The plasmas described in this way are expected to have many properties in common with the actual quark–gluon plasma created in heavy-ion collisions, and the latter has indeed been found

to be strongly coupled at the experimentally accessible temperatures somewhat above the critical temperature [6–12].

Heavy quarkonia are among the most sensitive probes used in the experimental study of the quark–gluon plasma and its properties. Depending on the size of the quarkonium state and on the temperature of the plasma, the heavy quark and antiquark may be screened from each other, affecting the production rates of heavy quarkonia in heavy-ion collisions, see [13] for an early, influential reference. The static potential of two infinitely heavy quarks and their free energy play a central role in the theoretical description of color screening and its consequences for heavy quarkonia. These two quantities arise naturally in effective field theories which, due to the separation of different energy scales, provide a systematic way of dealing with phenomena involving heavy quarks both in vacuum and at finite temperature, see for instance [14, 15]. A static pair corresponds to the simplest equilibrium situation one can address in this context: a quark and an antiquark, both infinitely heavy, at a given distance and being at rest with respect to an infinitely extended plasma. Even for this simple situation, the ab initio calculation of the free energy or the potential is not a simple task since the presence of a strongly coupled plasma requires a nonperturbative framework. Lattice gauge theory has been used to calculate the free energy of a static quark pair for QCD and quenched versions of it, see for example [16–20].

The AdS/CFT correspondence offers a new and simple method to calculate the free energy of a heavy quark–antiquark pair and various related quantities in gauge theory plasmas. Besides the simplicity of the calculation, which can even be done analytically in some cases, the advantage of the holographic description is that it can be applied also to situations which are in general prohibitively difficult to attack using lattice gauge theory. Examples include dynamical processes with moving quarks, hydrodynamic properties of the medium like transport coefficients, or plasmas with a finite chemical potential. Although an exact holographic dual of QCD is not known, the method promises considerable insight into the dynamics of strongly coupled gauge theory plasmas in general, not least because many strongly coupled systems appear to share universal features. The calculation of the free energy of a static pair in an $\mathcal{N} = 4$ SYM plasma [21, 22] was among the first applications of the AdS/CFT correspondence. In the meantime, the free energy of a heavy quark–antiquark pair has been addressed in the AdS/CFT framework for various theories and kinematic situations in different approximations, mostly following the ideas and prescriptions of those two early studies. The corresponding papers are far too numerous to be cited here comprehensively; for a partial list of references see for example [4].

In the AdS/CFT framework, heavy quarks have a simple description as endpoints of macroscopic open strings. These endpoints can move on the 3+1 dimensional boundary of the five-dimensional AdS space, which can be identified with the physical Minkowski space. The string connecting the quark and antiquark hangs down into the bulk, that is into the fifth dimension of the AdS space. (The S_5 factor in the metric does not play an important role for the observables that we consider here.) A single heavy quark at rest corresponds to an open string hanging down from the boundary into the black hole horizon. The dynamics of the quark–antiquark pair or of a single quark is then determined by the classical dynamics of the open string in the AdS background, encoded in its Nambu–Goto

action.

In the present work, we reconsider the holographic calculation of the free energy of the heavy quark–antiquark pair in a thermal medium. In particular, we point out an issue with the most commonly used prescriptions for the UV renormalization in that calculation. Following [21, 22], the UV divergence in the action of a string connecting a heavy quark pair is usually cured by subtracting the action of two strings hanging down into the horizon, corresponding to two non-interacting quarks. However, this prescription leads to an unphysical temperature dependence of the free energy at small distances. The same is true for several other prescriptions commonly used in the literature. We will discuss how the temperature dependence enters through the corresponding subtraction terms. We will then advocate a different, consistent subtraction which avoids this problem. Let us note here that essentially equivalent consistent subtractions have been used before in the finite-temperature context, see[1] [23–27], and the authors of [28] comment as a side remark that using a temperature-dependent renormalization is not correct. However, to the best of our knowledge the full implications of the details of the renormalization procedure and the distinctions between the quantities resulting from different procedures have not yet been discussed before. Here, we fill this apparent gap in the literature and, in particular, we study thermodynamic quantities related to the free energy that crucially require the use of a temperature-independent renormalization, namely the entropy and the internal energy of the pair. We will show that with the consistent UV subtraction the free energy as calculated in the AdS/CFT framework is in good qualitative agreement with the lattice results. We will also point out that the most commonly used subtraction procedure gives rise to the binding energy of the pair rather than its free energy, and we will discuss the marked differences between these two quantities. As a byproduct of our study we obtain a consistent definition of the free energy, the entropy, and the internal energy of a single heavy quark in the holographic framework. We will also compare the AdS/CFT results for these quantities to lattice results.

We will consider the observables just described in various theories. At finite temperature, despite their different particle content, QCD in the deconfined phase and $\mathcal{N} = 4$ SYM share some essential properties, see for example [4]. This is in stark contrast to the situation at vanishing temperature where these two theories are very different. In the following, we will therefore always have the quark–gluon plasma phase of QCD in mind when we apply the holographic duality. But also in the plasma phase, QCD differs from $\mathcal{N} = 4$ SYM in various respects. The most important difference has its origin in the conformal invariance of $\mathcal{N} = 4$ SYM. Although the conformality of $\mathcal{N} = 4$ SYM is broken at finite temperature, the temperature is the only dimensionful scale. The behavior of such a plasma at different temperatures therefore obeys a scaling of all dimensionful quantities with the appropriate powers of temperature. In QCD, the properties of the plasma depend on temperature in a more complicated way due to the presence of other energy scales characterizing the dynamics, in particular up to temperatures of several times the critical temperature. In holography, non-conformal theories closer to QCD can be obtained by introducing defor-

[1] Although we have thoroughly searched the literature that list may be not exhaustive.

mations of pure AdS space. We will in this paper only discuss bottom-up approaches of this kind. The simplest way of constructing a non-conformal theory is to supplement, in an *ad hoc* way, the AdS-black hole metric dual to $\mathcal{N} = 4$ SYM with suitable factors, often chosen of soft-wall type [29], see for example [30, 31]. In general, such a metric does not solve the equations of motion of any five-dimensional Einstein–Hilbert action, and thus may lead to inconsistencies. A more consistent method is to introduce additional scalar fields in the five-dimensional bulk of the AdS space [32]. These models can be constructed such that the backreaction of the scalar field on the metric changes the behavior only in the IR region of the dual field theory, and the metric remains asymptotically AdS. One can in fact design specific holographic models of strongly coupled QCD along these lines. In the present work, instead of considering one specific model resembling QCD, we want to take a different approach by studying families of consistent non-conformal models. In these models one can investigate the general effect of non-conformal deformations and look for universal properties common to large classes of non-conformal theories at strong coupling. We will indeed find indications for such universal behavior in the observables that we study.

Our paper is organized as follows. In sec. 2 we review the holographic calculation of a temporal Wegner–Wilson loop corresponding to a macroscopic string connecting a static, heavy quark–antiquark pair in a thermal medium. We use a general AdS-type metric that encompasses the holographic dual of $\mathcal{N} = 4$ SYM and the non-conformal models we want to consider. Sec. 3 deals with the computation of the free energy of the heavy quark–antiquark pair in the holographic framework. Here, we discuss in particular the temperature dependence of different renormalization prescriptions used in this framework and argue that the free energy should be independent of temperature at small distances. We then show how the free energy and the binding energy are obtained as results of different renormalization procedures. We illustrate these general considerations for the case of $\mathcal{N} = 4$ SYM in sec. 4 where we compare the free energy to lattice QCD calculations on the one hand and to the binding energy on the other hand. Next, in sec. 5, we investigate how the introduction of non-conformality affects the free energy and the binding energy of the pair. In sec. 6 we use the fact that the free energy is a thermodynamic potential and compute the associated entropy and internal energy for $\mathcal{N} = 4$ SYM and for the non-conformal models. Finally, in sec. 7 we study the free energy and the associated entropy and internal energy of a single heavy quark in the strongly coupled plasmas described by our models. In particular, we look for universal effects of non-conformal deformations. We present our conclusions in sec. 8. Appendix A contains some technical details concerning the calculation of the entropy of the heavy pair.

2 String in general AdS-type metric

Let us first review the calculation of the string configuration holographically corresponding to a heavy quark–antiquark pair in a thermal medium. We will do this using a general form of the metric of the five-dimensional AdS-type space. The results for particular holographic theories, *i. e.* $\mathcal{N} = 4$ SYM and non-conformal models, are later obtained as special cases.

The most general form of the five-dimensional, asymptotically AdS metric g_{MN} compatible with translation invariance in the boundary directions $(t, \vec{x}) = (t, x^1, x^2, x^3) = (x^\mu)$ and $SO(3)$ invariance in $\vec{x}$ is given by

$$\mathrm{d}s^2 = \mathrm{e}^{2A(z)} \left(-h(z)\,\mathrm{d}t^2 + \mathrm{d}\vec{x}^2\right) + \frac{\mathrm{e}^{2B(z)}}{h(z)}\,\mathrm{d}z^2\,, \tag{2.1}$$

where $\mathrm{d}s^2 = g_{MN}\,\mathrm{d}X^M\,\mathrm{d}X^N$, and z is the fifth-dimensional, holographic coordinate.

All our model spacetimes are asymptotically AdS. This implies boundary conditions at $z = 0$ for the functions A, B, and h in the ansatz (2.1), namely

$$A(z) \sim \log\left(\frac{L_{\mathrm{AdS}}}{z}\right) \text{ as } z \to 0\,, \tag{2.2}$$

$$B(z) \sim \log\left(\frac{L_{\mathrm{AdS}}}{z}\right) \text{ as } z \to 0\,, \tag{2.3}$$

$$h(z = 0) = 1\,. \tag{2.4}$$

L_{AdS} sets the curvature scale of the AdS space. A zero in the 'blackening' function $h(z)$ signals the presence of a black hole (more precisely, a black brane extended in the t and $\vec{x}$ directions), and we denote its horizon position by z_{h}, that is $h(z_{\mathrm{h}}) = 0$. For the general metric (2.1) the Hawking temperature is [32, 33]

$$T = \frac{\mathrm{e}^{A(z_{\mathrm{h}})-B(z_{\mathrm{h}})}|h'(z_{\mathrm{h}})|}{4\pi}\,. \tag{2.5}$$

For simplicity, we will generically refer to asymptotically AdS spaces given by metrics with the above properties as 'AdS spaces'.

For the quantities that we want to compute, we will need to evaluate the expectation value of a rectangular Wegner–Wilson loop in the boundary theory. The holographic calculation of this quantity by means of a dual macroscopic open string with both endpoints on the boundary (representing an infinitely heavy quark–antiquark pair) is well known and can by now be found in textbooks such as [4]. In the following we present a brief outline of the calculation, concentrating on the points relevant for the discussion in the following sections.

The Wegner–Wilson-loop operator in the gauge-theory medium is defined as

$$W(\mathcal{C}) = \mathrm{tr}\,\mathcal{P}\exp\left(\mathrm{i}\oint_{\mathcal{C}} \mathrm{d}x^\mu A_\mu(x)\right)\,. \tag{2.6}$$

Here, $\mathcal{C}$ is a closed contour in spacetime, $A_\mu(x) = A^a_\mu(x)T^a$ is the non-Abelian gauge field where T^a are the generators in the representation that the trace is taken over. $\mathcal{P}$ denotes path ordering. For our purposes, the integration contour to consider is a rectangular contour $\mathcal{C}_{L,\mathcal{T}}$, composed of the timelike worldlines of length $\mathcal{T}$ of the heavy quarks and two small segments along the spacelike direction in which they are separated by the distance L. We choose the separation L to be in the $x = x^1$ direction. The limit $\mathcal{T} \to \infty$ of infinite

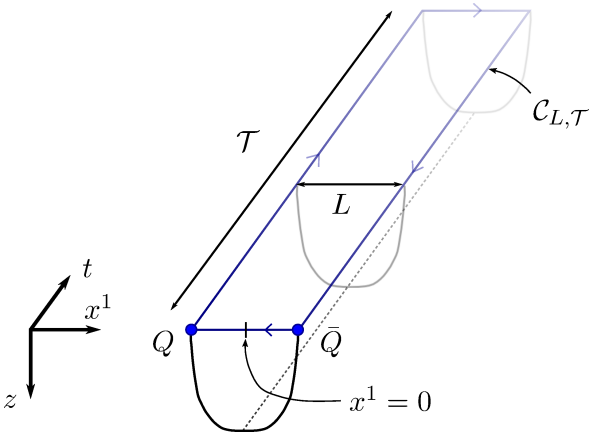

Figure 1. Sketch of a static quark–antiquark pair separated by a distance L along the boundary coordinate direction x^1. The quarks' worldlines are parallel to the time direction t, and the connecting string extends into the bulk coordinate direction z. Spacelike slices of the string worldsheet and the integration contour $\mathcal{C}_{L,\mathcal{T}}$ used in the integration for the Wegner–Wilson loop (2.6) are shown. The timelike edges of $\mathcal{C}_{L,\mathcal{T}}$ are of length $\mathcal{T}$ and coincide with the worldlines of the quarks. Eventually, the limit $\mathcal{T} \to \infty$ will be taken.

temporal extension is required for the quantities we want to study. Fig. 1 shows a sketch of this setup.

In the holographic description, the Wegner–Wilson loop is related to the Nambu–Goto action of an open string that hangs down into the bulk (fifth) dimension of the AdS space and whose endpoints trace out the contour of the loop situated at $z = 0$. The Nambu–Goto action is given by

$$S_{\mathrm{NG}} = -\frac{1}{2\pi\alpha'} \int \mathrm{d}^2\sigma \sqrt{-\det g_{ab}}\,. \tag{2.7}$$

The integral extends over the worldsheet of the string. $1/(2\pi\alpha')$ is the string tension and g_{ab} the induced metric on the worldsheet,

$$g_{ab} = g_{MN} \frac{\partial X^M}{\partial \sigma^a} \frac{\partial X^N}{\partial \sigma^b}\,, \qquad a, b = 0, 1\,, \tag{2.8}$$

where $X^M = (t, x, 0, 0, z(x))$ are the five-dimensional coordinates of the string worldsheet in the AdS space. We work in static gauge with $\sigma^0 = t$ and $\sigma^1 = x$.

In the following we will always assume that the Nambu–Goto action (2.7) captures the relevant dynamics of our problem to a good approximation. Depending on the model under consideration or on the approximation to full 10-dimensional string theory there can occur various corrections, among them couplings of further bulk fields to the string worldsheet. Our considerations would then obviously need to be modified correspondingly. Here, we consider only cases in which the Nambu–Goto action is a good approximation.

For the general metric (2.1), we derive the following explicit form of the Nambu–Goto action (2.7) for the string worldsheet bounded by $\mathcal{C}_{L,\mathcal{T}}$,

$$S_{\mathrm{NG}}[\mathcal{C}_{L,\mathcal{T}}] = -\frac{\mathcal{T}}{2\pi\alpha'} \int_{-L/2}^{L/2} \mathrm{d}x\, \mathrm{e}^{2A} \sqrt{h \left(1 + \frac{\mathrm{e}^{2B-2A}}{h}\, z'^2\right)}\,, \tag{2.9}$$

where A, B, and h depend on $z(x)$ and we have performed the trivial t-integration. The function $z(x)$ describes the shape of the string hanging into the bulk, and z' denotes the derivative with respect to x. The endpoints of the string are located at the boundary, $z\left(-\frac{L}{2}\right) = z\left(\frac{L}{2}\right) = 0$, and the solution is symmetric with respect to $x = 0$. From the above action one readily derives the equation of motion for the embedding $z(x)$, which for $x \geq 0$ gives

$$z'(x) = -\mathrm{e}^{A(z)-B(z)} \sqrt{h(z)\left(\frac{\mathrm{e}^{4A(z)}h(z)}{\mathrm{e}^{4A(z_\mathrm{t})}h(z_\mathrm{t})} - 1\right)}\,. \tag{2.10}$$

One finds that the string descends into the bulk, reaching a turning point at $z = z_\mathrm{t}$ for $x = 0$, that is $z_\mathrm{t} = z(0)$, before symmetrically ascending again towards the boundary, as sketched in fig. 1. Using (2.10), the distance L can be expressed as a function of the turning point z_t,

$$L(z_\mathrm{t}) = 2\int_0^{L/2} \mathrm{d}x = 2\int_0^{z_\mathrm{t}} \frac{\mathrm{d}z}{-z'} = 2\int_0^{z_\mathrm{t}} \mathrm{d}z\, \mathrm{e}^{B-A}\left[h\left(\frac{\mathrm{e}^{4A}h}{\mathrm{e}^{4A_\mathrm{t}}h_\mathrm{t}} - 1\right)\right]^{-1/2}. \tag{2.11}$$

Here, functions with a subscript 't' are to be evaluated at the turning point z_t.

As first observed in [21, 22] for the case of $\mathcal{N} = 4$ SYM, real-valued solutions for the string configuration can only be found for distances L up to a certain value L_s that depends on the temperature. The same holds in non-conformal models where the value of L_s then also depends on the chosen metric. For a given model the situation is the following. One can uniquely parametrize the possible string configurations by their turning point z_t. For each L with $0 \leq L < L_\mathrm{s}$ there are two possible string configurations. The one staying further away from the black hole horizon turns out to have the smaller free energy, while the one coming closer to the horizon has a larger free energy and is thus energetically disfavored and unstable as we will discuss in more detail in sec. 4 below. As L is increased the two solutions approach each other and at $L = L_\mathrm{s}$ merge into a single solution. None of the solutions touches the horizon except for the unstable configuration in the limit $L \to 0$ (although the contrary is sometimes claimed in the literature). L_s is the maximally possible distance at which the quark and antiquark form a bound state connected by a string of the type described above. For larger distances they are screened by the thermal medium, and we hence call L_s the screening distance. It should not be confused with the Debye screening length that characterizes the exponential falloff of the interaction between the quark and antiquark at still larger distances. The screening distance L_s can in a first approximation be considered as the point where the transition from an approximately Coulombic to an exponentially damped interaction between the quark and antiquark takes place. We will in the present paper only consider inter-quark distances smaller than L_s in the respective models. In the holographic description one would need to take into account more complicated string configurations to describe the large-distance behavior beyond L_s, see for example the discussions in [34, 28]. In the following, we will concentrate on the energetically favored string configurations, but our general considerations will apply also to the energetically disfavoured configurations.

In our discussion below we will evaluate the Nambu–Goto action (2.7) for a macroscopic string propagating in the five-dimensional AdS spacetime. It contains the parameter α',

and our general metric (2.1) always includes a factor $L^2_{\rm AdS}$ due to the boundary conditions (2.2) and (2.3) satisfied by all our models. We define

$$\sqrt{\lambda} = \frac{L^2_{\rm AdS}}{\alpha'} \tag{2.12}$$

for the combination of $L_{\rm AdS}$ and α' that will generically appear in our observables. In the holographic dual of $\mathcal{N} = 4$ SYM, λ coincides with the 't Hooft coupling $\lambda = g^2_{\rm YM} N_{\rm c}$. However, when we consider non-conformal models obtained by non-conformal deformations of the bulk theory we have less precise information about the dual boundary theory. In particular, we do not know its Lagrangian and its (gauge) field content. As a consequence, we cannot be sure of the exact meaning of λ in the boundary theory. In any case, it stands to reason that also in our non-conformal models λ still is a proxy for the coupling strength in the boundary field theory. In phenomenological applications to the quark–gluon plasma one would have to dial a particular value for λ in a given model with a non-conformal deformation. In practice this amounts to treating λ as an additional free parameter of the model, with the caveat that it should be large for the duality to be applicable in the approximation that we use. The observables that we consider below will always contain a factor $\sqrt{\lambda}$. Since in this work we are mainly interested in their qualitative behavior we will divide out that overall factor in plots showing these quantities.

3 Free energy versus binding energy of a heavy quark pair

We now turn to the heavy quark–antiquark free energy. From the field-theory perspective, the Wegner–Wilson loop considered in the previous section is a gauge-invariant object that in particular encodes the free energy of the $Q\bar{Q}$ pair. To wit, in the limit of infinite temporal extent of the contour, $\mathcal{T} \to \infty$, we have the relation

$$\left\langle W(\mathcal{C}_{L,\mathcal{T}}) \right\rangle \sim \exp\left(-\mathrm{i} F_{Q\bar{Q}}(L)\mathcal{T}\right) , \qquad \mathcal{T} \to \infty , \tag{3.1}$$

where $F_{Q\bar{Q}}(L)$ is the $Q\bar{Q}$ free energy [35–37].[2] The expectation value is to be taken for a thermal state of the medium surrounding the quarks. This introduces the dependence of $F_{Q\bar{Q}}$ in (3.1) on the temperature T of the medium. The relation (3.1) holds up to an infinite renormalization constant that we will discuss in the context of the holographic computation below.

The problem now is to compute the expectation value of the Wegner–Wilson loop on the gravity side. The basic prescription was given in [41, 42]. From the bulk perspective, the integration contour $\mathcal{C}$ coincides with the boundary of the worldsheet of the string dual

[2] More precisely, recent studies starting with [38] have argued that in QCD the real-time Wegner–Wilson loop in the limit $\mathcal{T} \to \infty$ gives rise to an effective quark potential that is in general complex. However, the real part of this potential appears to coincide [39] with the $Q\bar{Q}$ (singlet) free energy that is defined from a Euclidean-time Wegner–Wilson loop. Indeed, this seems to be confirmed by lattice QCD calculations which reconstruct the real-time potential from the Euclidean-time spectral function (see *e. g.* [40]). Therefore, we call the quantity extracted from the real-time Wegner–Wilson loop via the holographic procedure discussed in the following the $Q\bar{Q}$ free energy, and, in accordance with the literature, interpret it as such.

to the quarks, as discussed in the previous section. The expectation value of the Wegner–Wilson loop is then related to the on-shell string action by

$$\big\langle W(\mathcal{C})\big\rangle \sim \exp\left(\mathrm{i}S_{\mathrm{NG}}[\mathcal{C}]\right) , \tag{3.2}$$

with $S_{\mathrm{NG}}[\mathcal{C}]$ the extremal Nambu–Goto action of the string. This is the saddle-point approximation of the more general statement where on the right-hand side we would have a path integral over all string configurations in the bulk with the prescribed boundary conditions [42].

From equations (3.1) and (3.2) it follows that the $Q\bar{Q}$ free energy can be computed holographically from

$$F_{Q\bar{Q}}(L) \sim -\frac{S_{\mathrm{NG}}[\mathcal{C}_{L,\mathcal{T}}]}{\mathcal{T}} , \qquad \mathcal{T}\to\infty . \tag{3.3}$$

This relation still needs to be renormalized. For that we introduce a regularization on the gravity side as follows. For our system, an expression for $S_{\mathrm{NG}}[\mathcal{C}_{L,\mathcal{T}}]$ can be obtained by plugging $z'(x)$ from the equation of motion (2.10) into the action functional (2.9). After rewriting the integration over the coordinate x as an integration over the bulk coordinate z we obtain

$$S_{\mathrm{NG}}[\mathcal{C}_{L,\mathcal{T}}] = -\frac{\mathcal{T}}{\pi\alpha'}\int_0^{z_{\mathrm{t}}} \mathrm{d}z\, \mathrm{e}^{A+B}\sqrt{\frac{\mathrm{e}^{4A}h}{\mathrm{e}^{4A}h-\mathrm{e}^{4A_{\mathrm{t}}}h_{\mathrm{t}}}} , \tag{3.4}$$

using again a subscript 't' on functions to indicate their evaluation at the turning point z_{t}. Recall from (2.11) that the turning point z_{t} is directly related to the $Q\bar{Q}$ distance L. As it stands, the expression (3.4) is divergent. For all models whose metric approaches the AdS metric asymptotically, as $z\to 0$, the first factor e^{A+B} is asymptotic to L^2_{AdS}/z^2, whereas the square root approaches unity asymptotically. Thus, we have a divergence from the lower integral limit, which can be regularized by restricting the integration to start a small distance ε away from the boundary. We thus write for the regularized action

$$S^{(\mathrm{reg})}_{\mathrm{NG}}[\mathcal{C}_{L,\mathcal{T}}] = -\frac{\mathcal{T}}{\pi\alpha'}\int_{\varepsilon}^{z_{\mathrm{t}}} \mathrm{d}z\, \mathrm{e}^{A+B}\sqrt{\frac{\mathrm{e}^{4A}h}{\mathrm{e}^{4A}h-\mathrm{e}^{4A_{\mathrm{t}}}h_{\mathrm{t}}}} \sim -\frac{\mathcal{T}L^2_{\mathrm{AdS}}}{\pi\alpha'}\left(\frac{1}{\varepsilon}+\ldots\right) . \tag{3.5}$$

The divergence is a pole $\sim 1/\varepsilon$. It appears because the string endpoints should be situated at the boundary $z=0$, which is the holographic realization of the infinite-quark-mass limit [42]. Subtracting an appropriate (infinite) quantity ΔS containing the $1/\varepsilon$ pole, we can write (3.3) in an operational form for the computation of the renormalized free energy,

$$F^{(\mathrm{ren})}_{Q\bar{Q}}(L) = \lim_{\mathcal{T}\to\infty}\left(-\frac{S^{(\mathrm{reg})}_{\mathrm{NG}}[\mathcal{C}_{L,\mathcal{T}}]-\Delta S}{\mathcal{T}}\right) . \tag{3.6}$$

This expression tacitly includes the limit $\varepsilon\to 0$ that removes the regulator. Henceforth, we will drop the specification 'ren' and simply write $F_{Q\bar{Q}}$ for the renormalized free energy; likewise, we will drop the superscript 'reg'. It remains to specify the subtraction ΔS.

There are two main choices for ΔS that have been used in the literature:

- Expectation values of Wegner–Wilson loops at finite temperature in AdS/CFT were first computed in [21] and [22]. There, the subtraction is chosen as twice the action of a straight string stretching from the boundary at $z = 0$ to the black hole horizon at $z = z_\mathrm{h}$. This is the commonly used procedure in the literature, it is also used in non-conformal theories, see for instance [4] and references therein.

- In [43] the real part of the Nambu–Goto action for infinite $Q\bar{Q}$ distance L is subtracted. Given that there are no real solutions to the string equation of motion for $L > L_\mathrm{s}$, the authors of [43] continue the string configuration into the complex domain.

These two procedures differ from each other only at non-zero temperature. For $T \to 0$ both reduce to the procedure used in the first papers on the computation of the heavy-quark free energy (or heavy-quark potential) at $T = 0$ in AdS/CFT [41, 42].

We argue in the following that neither of these procedures is appropriate for the calculation of the $Q\bar{Q}$ free energy at finite temperature. Let us first discuss our expectations for this quantity on the field theory side. For small distances L, we expect the temperature T as well as a possible deformation scale to have negligible effect on the $Q\bar{Q}$ interaction. The physical reason is that the corresponding scales are widely separated: the thermal excitations of the medium have typical wavelengths of order $1/T$ and hence cannot resolve the interaction of the $Q\bar{Q}$ pair at very small distances $L \ll 1/T$. In other words, the physics in the UV region of small distances cannot be affected by the thermal scale T. This consideration is supported by data from lattice QCD, *e. g.* [19, 20], where indeed for $LT \ll 1$ the free energy becomes independent of T, see also [17]. Now consider (3.6) for the holographic computation of the free energy. The first term $S_\mathrm{NG}[\mathcal{C}_{L,\mathcal{T}}]$ becomes independent of any scale other than L for very small L. This is straightforward to see in the bulk picture for all spacetimes that are asymptotically AdS, which in particular includes all models that we consider here. Note that small L implies a small turning point z_t. (Recall that of the two string configurations corresponding to a given L we choose the one with the turning point closer to the boundary, *i. e.* the one with smaller z_t. We will explicitly verify below that indeed that string configuration is energetically preferred over the one with larger z_t.) Thus, a string corresponding to very small L only probes the part of the spacetime that is essentially fixed by the boundary conditions and does not depend on the temperature or a possible deformation parameter, which manifest themselves significantly only deeper in the bulk. We will numerically confirm this bulk argument when discussing the free energy in the following sections.

Now, if $F_{Q\bar{Q}}$ should, for small L, not depend on T (nor a potential deformation scale), then also the subtraction ΔS should not depend on these scales either. Moreover, ΔS should not depend on L. We therefore advocate a minimal choice ΔS_min that just subtracts the $1/\varepsilon$ pole in the regularized Nambu–Goto action (3.5). Explicitly, we choose

$$\Delta S_\mathrm{min} \equiv -\frac{\mathcal{T} L_\mathrm{AdS}^2}{\pi\alpha'} \int_\varepsilon^\infty \frac{\mathrm{d}z}{z^2} = -\frac{\mathcal{T} L_\mathrm{AdS}^2}{\pi\alpha'} \frac{1}{\varepsilon} \,. \tag{3.7}$$

As the free energy is defined only up to an overall constant offset, one could of course modify ΔS_min by an additive constant as long as it is T-independent. Our choice of ΔS_min

can be used in all models that we will consider here, and more generally in any model for which the metric asymptotically reduces to AdS. The choice (3.7) ensures that the right-hand side of (3.6) does in fact yield the free energy, and that the latter does not depend on T (and neither on a possible deformation scale) for small $Q\bar{Q}$ distances L.

Consequently, using formula (3.6) with the subtraction (3.7) we find the following expression for the free energy in terms of a string in our general AdS metric,

$$\frac{\pi F_{Q\bar{Q}}(z_{\rm t})}{\sqrt{\lambda}} = \int_0^{z_{\rm t}} {\rm d}z \left[\frac{{\rm e}^{A+B}}{L_{\rm AdS}^2} \sqrt{\frac{{\rm e}^{4A}h}{{\rm e}^{4A}h - {\rm e}^{4A_{\rm t}}h_{\rm t}}} - \frac{1}{z^2} \right] - \frac{1}{z_{\rm t}} \,. \tag{3.8}$$

Here, we have used the abbreviation $\sqrt{\lambda} = L_{\rm AdS}^2/\alpha'$, see (2.12).

As we have pointed out in the introductory section, there have been studies in the literature using a subtraction procedure essentially equivalent to the one that we have just described, see for example [23–27]. However, to the best of our knowledge the consequences of different choices of subtraction have not been discussed in depth so far. In particular, the different choices for the subtraction give rise to different physical quantities as we will describe momentarily. Our aim here is to clarify these differences. In the following sections, we will then compute further quantities the definition of which crucially depends on the correct (temperature-independent) subtraction procedure in the computation of the free energy.

The quantity obtained via the most commonly used subtraction procedure (the first one in the list above) is the difference of the string action of the 'U'-shaped string connecting the quarks and twice the string action of a straight string stretching from the boundary to the horizon,

$$E_{Q\bar{Q}}(L) = \lim_{\mathcal{T}\to\infty} \left(- \frac{S_{\rm NG}[\mathcal{C}_{L,\mathcal{T}}] - 2S_{\rm NG}[\text{straight string}]}{\mathcal{T}} \right) . \tag{3.9}$$

In a general metric of the form (2.1) the Nambu–Goto action for a worldsheet corresponding to a static straight string hanging down from the boundary to the horizon is given by

$$S_{\rm NG}[\text{straight string}] = -\frac{\mathcal{T}}{2\pi\alpha'} \int_0^{z_{\rm h}} {\rm d}z \, {\rm e}^{A+B} \,. \tag{3.10}$$

It can be regularized in the same way as $S_{\rm NG}[\mathcal{C}_{L,\mathcal{T}}]$ above by cutting off the integral at a distance ε away from the boundary. Its divergence for $\varepsilon \to 0$ is found in analogy to (3.5),

$$S_{\rm NG}^{(\rm reg)}[\text{straight string}] = -\frac{\mathcal{T}}{2\pi\alpha'} \int_\varepsilon^{z_{\rm h}} {\rm d}z \, {\rm e}^{A+B} \sim -\frac{\mathcal{T} L_{\rm AdS}^2}{2\pi\alpha'} \left(\frac{1}{\varepsilon} + \dots \right) . \tag{3.11}$$

Hence, its divergent part equals $\Delta S_{\rm min}/2$. We will again drop the superscript 'reg' in our notation.

Now the quantity $E_{Q\bar{Q}}(L)$ in (3.9) can be understood as a difference of free energies. Namely, by inserting a zero in the form $-\Delta S_{\rm min} + \Delta S_{\rm min}$ with the minimal $\Delta S_{\rm min}$ defined in (3.7) we can reinterpret this quantity as the difference of two finite quantities,

$$\begin{aligned} E_{Q\bar{Q}}(L) &= \lim_{\mathcal{T}\to\infty} \left[- \frac{\big(S_{\rm NG}[\mathcal{C}_{L,\mathcal{T}}] - \Delta S_{\rm min}\big) - \big(2S_{\rm NG}[\text{straight string}] - \Delta S_{\rm min}\big)}{\mathcal{T}} \right] \\ &= F_{Q\bar{Q}} - F_{Q\,;\,\bar{Q}} \,, \end{aligned} \tag{3.12}$$

where we have used (3.6) and the analogous relation for the free energy of two non-interacting heavy quarks, which we denote by $F_{Q\,;\bar{Q}}$, that is

$$F_{Q\,;\bar{Q}} = \lim_{\mathcal{T}\to\infty}\left(-\frac{2S_{\mathrm{NG}}[\text{straight string}] - \Delta S_{\mathrm{min}}}{\mathcal{T}}\right) . \tag{3.13}$$

This quantity can be written as $F_{Q\,;\bar{Q}} = 2F_Q$ where we may call F_Q the free energy of a single heavy quark. More explicitly, in our general AdS metric (2.1) we obtain F_Q as

$$\frac{\pi F_Q}{\sqrt{\lambda}} = \frac{1}{2}\left[\int_0^{z_{\mathrm{h}}} \mathrm{d}z \left(\frac{\mathrm{e}^{A+B}}{L^2_{\mathrm{AdS}}} - \frac{1}{z^2}\right) - \frac{1}{z_{\mathrm{h}}}\right] , \tag{3.14}$$

where we have again used the abbreviation $\sqrt{\lambda} = L^2_{\mathrm{AdS}}/\alpha'$. We will discuss this single-quark free energy further in sec. 7.

Let us turn back to $E_{Q\bar{Q}}(L)$. We see from (3.12) that $E_{Q\bar{Q}}(L)$ is an energy difference. It vanishes when the free energy of the interacting $Q\bar{Q}$ pair equals the free energy of a pair of non-interacting heavy quarks. We can thus interpret $E_{Q\bar{Q}}(L)$ (or more precisely, its negative) as the binding energy of the $Q\bar{Q}$ pair. Explicitly, for the binding energy we obtain the relation

$$\frac{\pi E_{Q\bar{Q}}(z_{\mathrm{t}})}{\sqrt{\lambda}} = \int_0^{z_{\mathrm{t}}} \mathrm{d}z\, \frac{\mathrm{e}^{A+B}}{L^2_{\mathrm{AdS}}}\left[\sqrt{\frac{\mathrm{e}^{4A}h}{\mathrm{e}^{4A}h - \mathrm{e}^{4A_{\mathrm{t}}}h_{\mathrm{t}}}} - 1\right] - \int_{z_{\mathrm{t}}}^{z_{\mathrm{h}}} \mathrm{d}z\, \frac{\mathrm{e}^{A+B}}{L^2_{\mathrm{AdS}}} . \tag{3.15}$$

The binding energy has been extensively studied (often as a 'finite-temperature quark–antiquark potential') by means of the gauge/gravity duality, see for instance [21, 22, 44, 23, 45–49]. These references include investigations in $\mathcal{N} = 4$ SYM (in the strict limit of infinite 't Hooft coupling λ as well as including first-order corrections in an expansion in $1/\lambda$ [48]) and in models with non-conformal deformation, at vanishing and non-zero temperature, and with the $Q\bar{Q}$ pair stationary or moving with respect to the rest frame of the background medium (including analyses of the dependence on the angle of the $Q\bar{Q}$ dipole to its velocity [45]). Furthermore, $E_{Q\bar{Q}}$ has been studied in holographic models of anisotropic strongly coupled plasma [50, 51], as well as at non-zero chemical potential in $\mathcal{N} = 4$ SYM [52] and non-conformal models [53].

We will see in the following sections that the behavior of the binding energy is fundamentally different from that of the free energy. Moreover, we will find that the free energy in $\mathcal{N} = 4$ SYM, as in the non-conformal models, behaves qualitatively like the $Q\bar{Q}$ free energy computed in lattice QCD, whereas the binding energy does not. This corroborates our general arguments for the use of the subtraction (3.7) for the computation of the free energy.

4 Free energy and binding energy in $\mathcal{N} = 4$ supersymmetric Yang–Mills theory

In the previous section we have obtained expressions for the $Q\bar{Q}$ free energy $F_{Q\bar{Q}}$ and binding energy $E_{Q\bar{Q}}$ in general holographic models, see (3.8) and (3.15), respectively. Now

we want to study the properties of these two quantities for the simplest case, namely $\mathcal{N}=4$ SYM whose gravity dual is given by pure AdS-black hole space. We will find the general behavior of the free energy to be in qualitative agreement with the behavior found in lattice QCD.

As is well known, $\mathcal{N}=4$ supersymmetric Yang–Mills theory at non-zero temperature in the limits of large number of colors and large 't Hooft coupling can be described by a classical gravity theory with the AdS_5-Schwarzschild metric

$$\begin{aligned} \mathrm{d}s^2 &= \frac{L_{\mathrm{AdS}}^2}{z^2}\left(-h(z)\,\mathrm{d}t^2 + \mathrm{d}\vec{x}^2 + \frac{1}{h(z)}\,\mathrm{d}z^2\right), \\ h(z) &= 1-\frac{z^4}{z_{\mathrm{h}}^4}\,. \end{aligned} \tag{4.1}$$

In other words, for $\mathcal{N}=4$ SYM the functions A and B in the general metric (2.1) are given by $A(z)=B(z)=\log(L_{\mathrm{AdS}}/z)$. At $z=z_{\mathrm{h}}$ there is a planar black-hole (black-brane) horizon whose associated Hawking temperature,

$$T=\frac{1}{\pi z_{\mathrm{h}}}\,, \tag{4.2}$$

is identified with the temperature of the boundary field theory.

In $\mathcal{N}=4$ SYM, we can evaluate the integrals in the formulae for $F_{Q\bar{Q}}$, $E_{Q\bar{Q}}$, and L explicitly. Using (3.15) for the binding energy $E_{Q\bar{Q}}(L)$ with the AdS-Schwarzschild metric (4.1), we obtain

$$\frac{\pi E_{Q\bar{Q}}(z_{\mathrm{t}})}{\sqrt{\lambda}} = -\frac{\sqrt{\pi}\,\Gamma\left(\frac{3}{4}\right)}{\Gamma\left(\frac{1}{4}\right)}\,{}_2\mathrm{F}_1\left(-\frac{1}{2},-\frac{1}{4};\frac{1}{4};\frac{z_{\mathrm{t}}^4}{z_{\mathrm{h}}^4}\right)\frac{1}{z_{\mathrm{t}}}+\frac{1}{z_{\mathrm{h}}}\,, \tag{4.3}$$

where ${}_2\mathrm{F}_1$ is the (Gaußian) hypergeometric function. An equivalent formula has been obtained in [54]. Note that, working in $\mathcal{N}=4$ SYM, $\sqrt{\lambda}$ which we defined as a shorthand for the ratio of bulk quantities $L_{\mathrm{AdS}}^2/\alpha'$ is in fact the 't Hooft coupling $\sqrt{\lambda}=g_{\mathrm{YM}}^2 N_{\mathrm{c}}$.

The temperature-dependent term $1/z_{\mathrm{h}}$ in (4.3) is entirely due to the contribution $2S_{\mathrm{NG}}[\text{straight string}]$ of the straight strings stretching from the boundary to the horizon, see (3.9). It is due to this term that $E_{Q\bar{Q}}$ depends on T for small inter-quark distances. As discussed above, this should not be the case for the free energy $F_{Q\bar{Q}}$, and $F_{Q\bar{Q}}$ indeed lacks that term. Explicitly, we find from (3.8) with the metric (4.1)

$$\frac{\pi F_{Q\bar{Q}}(z_{\mathrm{t}})}{\sqrt{\lambda}} = -\frac{\sqrt{\pi}\,\Gamma\left(\frac{3}{4}\right)}{\Gamma\left(\frac{1}{4}\right)}\,{}_2\mathrm{F}_1\left(-\frac{1}{2},-\frac{1}{4};\frac{1}{4};\frac{z_{\mathrm{t}}^4}{z_{\mathrm{h}}^4}\right)\frac{1}{z_{\mathrm{t}}}\,. \tag{4.4}$$

Comparing this to the binding energy $E_{Q\bar{Q}}$ we find that $F_{Q\bar{Q}}(L) < E_{Q\bar{Q}}(L)$ for any $T>0$, as $E_{Q\bar{Q}}$ in (4.3) has an additional positive contribution $1/z_{\mathrm{h}}$ (and L is in one-to-one correspondence to z_{t}). In the limit $T\to 0$, which is $z_{\mathrm{h}}\to\infty$ on the gravity side, $F_{Q\bar{Q}}$ and $E_{Q\bar{Q}}$ coincide.

We have expressed both the binding energy and the free energy in terms of the turning point z_{t}. The latter is related to the inter-quark distance L via the explicit relation

$$L(z_{\mathrm{t}}) = \frac{2\sqrt{\pi}\,\Gamma\left(\frac{7}{4}\right)}{3\,\Gamma\left(\frac{5}{4}\right)}\sqrt{1-\frac{z_{\mathrm{t}}^4}{z_{\mathrm{h}}^4}}\,{}_2\mathrm{F}_1\left(\frac{1}{2},\frac{3}{4};\frac{5}{4};\frac{z_{\mathrm{t}}^4}{z_{\mathrm{h}}^4}\right)z_{\mathrm{t}}\,, \tag{4.5}$$

derived from the general expression (2.11). This explicit form has also been obtained in [54].

For $T = 0$ it is possible to explicitly solve (4.5) for z_t and to compute $V_{Q\bar{Q}}(L) \equiv F_{Q\bar{Q}}(L) = E_{Q\bar{Q}}(L)$, the heavy quark–antiquark potential, analytically as a function of L,

$$V_{Q\bar{Q}}(L) = -\frac{4\pi^2\sqrt{\lambda}}{\Gamma^4\left(\frac{1}{4}\right) L}\,, \tag{4.6}$$

which has been first obtained in [42]. The strict proportionality $V_{Q\bar{Q}} \propto 1/L$ reflects the absence of any other dimensionful scale at $T = 0$.

There is another interesting fact that we would like to point out here. In $\mathcal{N} = 4$ SYM, the zero-temperature limit of the action (3.11) for a straight string stretching from the boundary to the horizon is, as a consequence of (4.1) and (4.2),

$$S_{\rm NG}[\text{straight string}]\big|_{\mathcal{N}=4,T=0} = -\frac{\mathcal{T} L^2_{\rm AdS}}{2\pi\alpha'} \int_\varepsilon^\infty \frac{\mathrm{d}z}{z^2}\,. \tag{4.7}$$

This quantity receives a contribution only from the lower limit of the integral and is thus fully given by the UV divergence of the straight string. It exactly coincides with one half of the minimal subtraction $\Delta S_{\rm min}$ that we advocate for the definition of $F_{Q\bar{Q}}$ in all models and for all temperatures, see (3.7). One could therefore think of the minimal subtraction for any asymptotically AdS metric as subtracting two straight strings corresponding to pure $\mathcal{N} = 4$ SYM at $T = 0$.

Let us now consider again general temperature T. In fig. 2, we plot $F_{Q\bar{Q}}(L)$ and $E_{Q\bar{Q}}(L)$ in $\mathcal{N} = 4$ SYM for varying temperature. Both $F_{Q\bar{Q}}(L)$ and $E_{Q\bar{Q}}(L)$ actually have two values for every distance L smaller than the screening distance $L_{\rm s}$, *i. e.*, both functions have two branches. This is a consequence of there being two string configurations for every distance $L < L_{\rm s}$, as discussed in sec. 2. The inset in fig. 2 displays the full $F_{Q\bar{Q}}(L)$ and $E_{Q\bar{Q}}(L)$, showing their lower and upper branches. The lower branches correspond to the string configurations that stay closer to the boundary. Since their free energy is smaller than that of the string configurations protruding farther into the bulk, they are energetically preferred. In addition, it turns out that the solutions that reach farther into the bulk possess runaway modes when subjected to small perturbations whereas the string configurations that stay closer to the boundary are stable against such perturbations [34]. From now on, we will always restrict our discussion to the stable, lower branches of both $F_{Q\bar{Q}}$ and $E_{Q\bar{Q}}$, and accordingly we have not plotted the upper branches in the main plot in fig. 2.

In fig. 2 we observe several characteristic properties of the free energy and the binding energy. For any value of T, the free energy $F_{Q\bar{Q}}$ becomes Coulombic at small inter-quark distances. This signals a restoration of conformality in the UV as the medium-induced scale T decouples. We further observe that the free energy becomes independent of T for small L. The binding energy $E_{Q\bar{Q}}$, on the other hand, depends on T also for small distances L as it contains an L-independent but T-dependent contribution. Fig. 2 also shows that the two energies exhibit a qualitatively different dependence on temperature. For $T = 0$, both $F_{Q\bar{Q}}(L)$ and $E_{Q\bar{Q}}(L)$ reduce to the same function, namely the zero-temperature potential

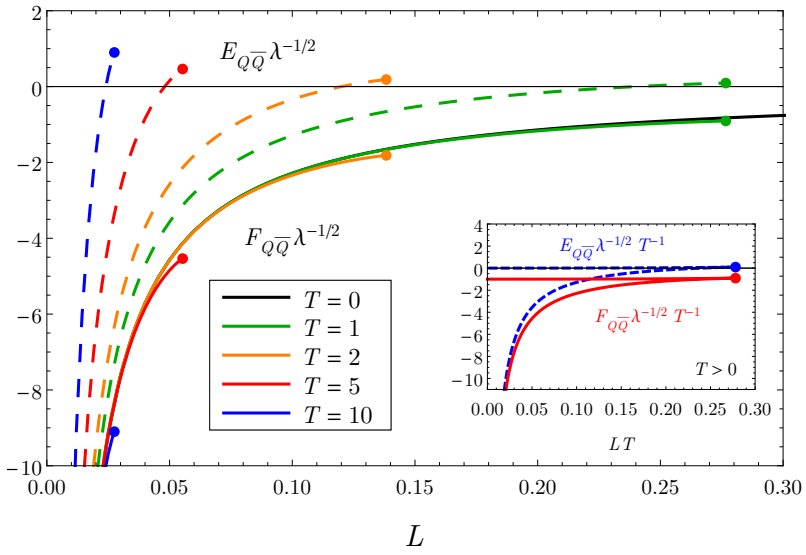

Figure 2. Free energy (solid curves) and binding energy (dashed curves) in $\mathcal{N} = 4$ SYM for varying temperature T, restricted to the stable branch (main plot) and including both the stable and the unstable branch (inset, $T > 0$), see text. For $T = 0$, both $F_{Q\bar{Q}}$ and $E_{Q\bar{Q}}$ reduce to the same Coulombic potential (solid black curve) given by (4.6). In the main plot, we express all dimensionful quantities in AdS units specified by $L_{\rm AdS} = 1$, and in the inset in units of temperature. The dots on the endpoints of the curves mark the screening distance.

given in (4.6). For increasing T, the free energy at fixed distance L becomes smaller as compared to the $T = 0$ limit, as is expected due to the screening of color charges in the medium. In contrast to that, $E_{Q\bar{Q}}$ increases with temperature. This behavior of $E_{Q\bar{Q}}$ is consistent with our interpretation of it as a (negative) binding energy. Due to increasing T, at a fixed distance L the modulus of the binding energy decreases. In other words, the binding of the quarks becomes weaker, as is natural in a hotter medium due to stronger screening of the interaction. Accordingly, also the screening distance becomes smaller for increasing T.

For any non-zero temperature, at some value $L_{\rm c} < L_{\rm s}$ of the inter-quark separation, the binding energy vanishes, $E_{Q\bar{Q}}(L_{\rm c}) = 0$. Thus, at this distance the free energy of the bound $Q\bar{Q}$ pair equals the free energy of an unbound $Q\bar{Q}$ pair, while for larger distances the free energy of an unbound pair is smaller than that of a bound pair. However, this does not necessarily imply that the $Q\bar{Q}$ pair dissociates at this length scale. In fact, the dynamic evolution of the string configurations (including in particular the breaking of the string) is beyond the approximation underlying (3.2) which was our starting point. The $Q\bar{Q}$ pair might well be metastable even beyond $L_{\rm c}$. For further discussion of this issue see, *e. g.*, [34].

At this point, we want to compare the qualitative behavior of the free energy in $\mathcal{N} = 4$ SYM to that of QCD. We clearly do not expect an exact quantitative agreement of $F_{Q\bar{Q}}$ in these two theories. However, the qualitative effect of the thermal medium on the heavy quark pair should be largely independent of the microscopic degrees of freedom present

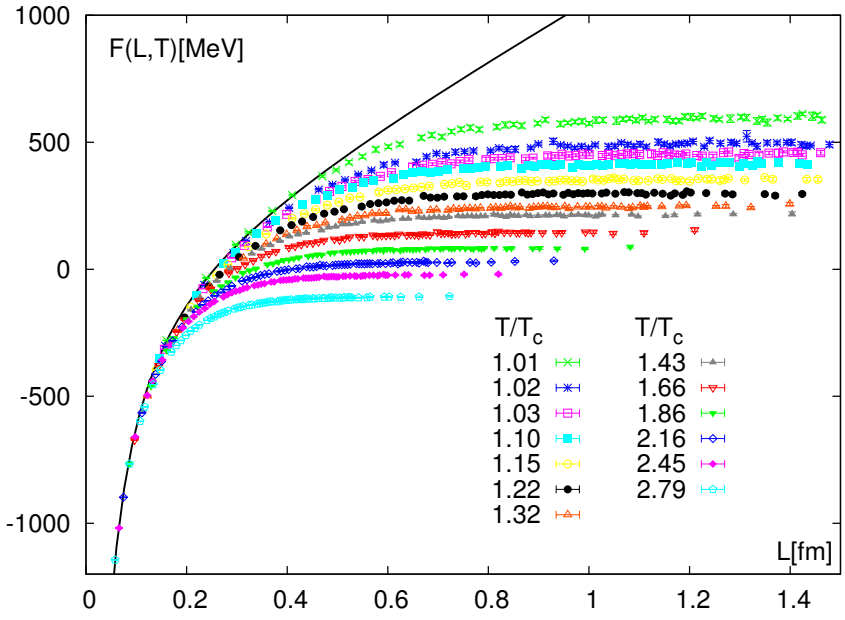

Figure 3. Heavy-quark free energy at various temperatures above T_c from a 2+1-flavor lattice QCD calculation [55]. The solid line shows the zero temperature heavy-quark potential [56].

in the two theories. In lattice QCD, the heavy-quark free energy can be extracted from a correlator of Polyakov loops. In fig. 3 we show lattice QCD results from [55] for 2+1-flavors with a physical strange quark mass and a pion mass of around 220 MeV using an improved staggered quark action [56]. For a discussion of the renormalization of the heavy quark free energies in lattice QCD see [57]. The temperature is varied and all chosen temperatures are above T_c. We note two characteristics of the behavior of the free energy. First, for small inter-quark distances L the free energy becomes independent of the temperature. Second, the free energy decreases with increasing T, *i. e.*, data points for some $T_2 > T_1$ always lie below those for T_1. Both these characteristics are also present in the free energy computed in $\mathcal{N} = 4$ SYM, as discussed above. Furthermore, they are also present in our non-conformal models that will be discussed in the next section. In contrast to this, the quantity $E_{Q\bar{Q}}$ behaves differently. It rather increases with increasing T. These findings further substantiate our general arguments regarding the choice (3.7) of the subtraction ΔS. Using it in (3.6) we indeed obtain the proper $Q\bar{Q}$ free energy.

5 Free energy and binding energy in non-conformal models

Next, we want to study the free energy and the binding energy of a heavy quark–antiquark pair in non-conformal theories, that is in theories in which the conformal symmetry is broken explicitly and not only by temperature. One can obtain such non-conformal theories as duals of suitable deformations of the AdS-Schwarzschild metric, typically containing one or more dimensionful parameters. Various non-conformal metrics have been discussed in the literature. Many of them aim at reproducing properties of the actual QCD plasma.

Here, we take a different approach and look for generic properties or universal behavior emerging in large classes of non-conformal models. To this end, we consider some prototype models which have been used before to study various observables in this spirit. In the first family of models (SW_T model) the non-conformality is introduced by hand, in the second set of models (consistently deformed 1-parameter models) it is associated with additional scalar fields in the bulk. In the latter models the metric solves the equations of motion for an Einstein–Hilbert–scalar action. We will briefly present the main properties of these models before we proceed to discussing the heavy quark pair in these backgrounds.

SW_T model. This model has been introduced in [30, 31] and is motivated by the soft-wall model at zero temperature [29] which had considerable success in describing various aspects of low-energy hadron physics. In the soft-wall model the AdS metric corresponding to $\mathcal{N} = 4$ SYM at zero temperature is multiplied by an overall warp factor of the form $\mathrm{e}^{c^2 z^2}$ with some deformation parameter c that determines the deviation from conformality. Applying the same procedure to the AdS-Schwarzschild metric corresponding to $\mathcal{N} = 4$ SYM at finite temperature one obtains the one-parameter family of models [30, 31]

$$\begin{aligned} \mathrm{d}s^2 &= \frac{L_{\mathrm{AdS}}^2\, \mathrm{e}^{c^2 z^2}}{z^2} \left(-h(z)\, \mathrm{d}t^2 + \mathrm{d}\vec{x}^2 + \frac{1}{h(z)}\, \mathrm{d}z^2 \right) , \\ h(z) &= 1 - \frac{z^4}{z_{\mathrm{h}}^4} , \end{aligned} \tag{5.1}$$

which we call the SW_T models, for 'soft wall-like models at finite temperature T' [58]. The horizon function h is the same as in the AdS-Schwarzschild metric (4.1), to which the metric (5.1) reduces in the limit $c \to 0$. Accordingly, the temperature of the boundary field theory in these models is defined as in $\mathcal{N} = 4$ SYM,

$$T = \frac{1}{\pi z_{\mathrm{h}}} . \tag{5.2}$$

Various observables concerning heavy quarks in the medium have been studied in the SW_T model, see for example [30, 24, 31, 59, 46]. A suitable choice for the parameter c of the model can be made by comparing observables to their phenomenological values in the actual quark–gluon plasma. In [46] it is argued that $0 \leq c/T \leq 2.5$ is a reasonable range for that choice.[3] The advantage of the SW_T model is its simplicity which even permits to compute some observables analytically. However, the metric (5.1) does not solve the equations of motion of any five-dimensional gravity action and is in that sense not consistent. As a consequence, the corresponding boundary theory does not satisfy general thermodynamic relations [31]. This problem is solved, though at the expense of a higher computational effort, by consistently deformed models to which we turn next. Despite its limitations, the SW_T model can be useful as a simple method to obtain a first impression of the behavior

[3] Note that in our warp factor, $\exp(c^2 z^2)$, the deformation parameter enters quadratically while [30] or [31, 46] have $\exp(cz^2)$ or $\exp\left(\frac{29}{20} cz^2\right)$, respectively. This is just a different notation, and it is straightforward to convert the corresponding values of the deformation parameter. The values quoted in the present paper apply to our choice of warp factor. We also recall that we are interested here in the general behavior under non-conformal deformations rather than in determining a precise value for the deformation.

of many observables under non-conformal deformations, as will also be confirmed by our results below.

Consistently deformed 1-parameter models. In general, it is preferable to study metrics that solve the Einstein equations of a gravity action, as the dual theories of such models are expected to exhibit consistent thermodynamic observables. One can construct non-conformal metrics of this kind by considering a bulk scalar field in AdS and its back-reaction on the AdS space [32]. This setup is described by the five-dimensional Einstein–Hilbert–scalar action

$$S = \frac{1}{16\pi G_{\rm N}^{(5)}} \int \mathrm{d}^5x \sqrt{-g} \left(\mathcal{R} - \frac{1}{2} \partial_M \phi \, \partial^M \phi - V(\phi) \right) , \tag{5.3}$$

where g is the determinant of the metric g_{MN}, $\mathcal{R}$ is the associated Ricci scalar, and $G_{\rm N}^{(5)}$ is the five-dimensional Newton constant. ϕ is the scalar that will induce the deformation away from conformality. The potential $V(\phi)$ for the scalar is assumed to contain as a constant term

$$V(\phi = 0) = -\frac{12}{L_{\rm AdS}^2} \tag{5.4}$$

which is twice the cosmological constant of an AdS space with curvature radius $L_{\rm AdS}$. For a vanishing scalar ϕ one obtains from (5.3) a pure AdS space (4.1) corresponding to $\mathcal{N} = 4$ SYM, and then only the temperature T is an additional parameter of the metric. Starting from the ansatz (2.1) for the general metric one can derive a coupled set of differential equations for the functions A, B, h, and V from the equations of motion of the action (5.3) [32]. One option is to start by specifying a potential V, see for example [32]. The coupled equations also permit another possibility, namely to specify the scalar profile in z and to calculate a suitable potential V [60]. We choose the latter option as it allows us to study models that come very close to the phenomenologically well-motivated soft-wall model. Also in this case it is possible to study large classes of metrics with one or more parameters. A two-parameter model of this kind has been proposed in [60]. In [58] a simplified 1-parameter version of that model has been devised which has the advantage that all functions in the metric can be expressed in closed form. We will in the following work with this 1-parameter model as it captures the main features relevant for our considerations. To obtain this model, one makes in the general metric (2.1) the ansatz

$$\begin{aligned} \phi(z) &= \sqrt{\frac{3}{2}} \kappa z^2 \,, \\ A(z) &= \log\left(\frac{L_{\rm AdS}}{z} \right) \end{aligned} \tag{5.5}$$

with a dimensionful deformation parameter $\kappa \geq 0$. The equations of motion of (5.3) then lead to

$$B(z) = \log\left(\frac{L_{\rm AdS}}{z} \right) - \frac{1}{4} \kappa^2 z^4 \,. \tag{5.6}$$

Also h and V can be obtained in closed form. We do not give these somewhat lengthy expressions as their details will not be relevant for the following discussion. With these

functions one obtains from (2.5) the temperature T in terms of the horizon position z_h in the 1-parameter model,

$$T = \frac{1}{\pi z_\mathrm{h}} \frac{\kappa^2 z_\mathrm{h}^4}{4} \frac{\mathrm{e}^{\kappa^2 z_\mathrm{h}^4/4}}{\mathrm{e}^{\kappa^2 z_\mathrm{h}^4/4} - 1} \,. \tag{5.7}$$

We will in the following consider typical values of the deformation parameter[4] in a similar range as in the SW_T model, $0 \leq \sqrt{\kappa}/T \leq 2.5$. In the limit $\kappa \to 0$ the 1-parameter model reduces to the pure AdS metric, and hence to $\mathcal{N} = 4$ SYM. Finally, the scalar ϕ in the 1-parameter model can be but need not be the dilaton. In the bottom-up models that we consider here, this is simply a choice one can make, and this alternative gives in fact rise to two distinct versions of the 1-parameter model, *cf.* a similar discussion in [60]. The difference between the two versions lies in the metric used in the calculation of the string configuration as outlined in sec. 2. The metric (2.1) with the functions A, B, and h just described is called the Einstein-frame metric, $g^{(\mathrm{E})}$. The string configuration has to be calculated using the string-frame metric, $g^{(\mathrm{s})}$, which is obtained by multiplying the Einstein-frame metric by a factor containing the dilaton,

$$g^{(\mathrm{s})} = \mathrm{e}^{\sqrt{\frac{2}{3}}\phi_\mathrm{dilaton}} \, g^{(\mathrm{E})} \,. \tag{5.8}$$

If ϕ is the dilaton, the string-frame metric hence differs from the Einstein-frame metric by the warp factor in (5.8) with the scalar profile in (5.5). In a model without a dilaton, *i. e.* if ϕ is some other scalar, the two frames coincide. To distinguish the models, we therefore speak of the 'string frame' version of the 1-parameter model if ϕ is the dilaton, and of the 'Einstein frame' version if ϕ is not the dilaton. The additional warp factor of the string-frame model makes this version of the 1-parameter metric rather similar to the SW_T metric, and the qualitative similarity of these two models will also be seen in our results below.

Let us now turn to the free energy of the heavy quark–antiquark pair in these non-conformal models. In fig. 4 we show the free energy $F_{Q\bar{Q}}$ at a fixed temperature and a large value of the dimensionless ratios of the deformation parameters and the temperature, $c/T = 2.5$ and $\sqrt{\kappa}/T = 2.5$ for the SW_T model and the 1-parameter models, respectively. For comparison, we have also plotted $F_{Q\bar{Q}}$ in $\mathcal{N} = 4$ SYM (black curve). Note that here and in some of the plots below we show all quantities in units of temperature, that is we use dimensionless ratios on the axes, here $F_{Q\bar{Q}}/T$ and LT. For non-conformal theories, however, the values of the observables for a different temperature T' cannot be read off from the same curve, instead one would have to regard the curve corresponding to an accordingly changed ratio of deformation parameter and temperature, c/T' or $\sqrt{\kappa}/T'$. We show such different curves only in some cases where we vary the deformation parameter. In spite of this slight complication in the interpretation of the curves, the representation in terms of dimensionless quantities appears to be the best way to compare different theories, that is models with different non-conformal deformation parameters c or κ.

[4] In the 1-parameter model it turns out that for a given temperature there is in fact a maximal deformation κ beyond which no solution can be found for that temperature [58], given by $(\sqrt{\kappa}/T)|_\mathrm{max} = 2.94$. Our choice of the deformation parameter $0 \leq \sqrt{\kappa}/T \leq 2.5$ covers almost all of the possible range.

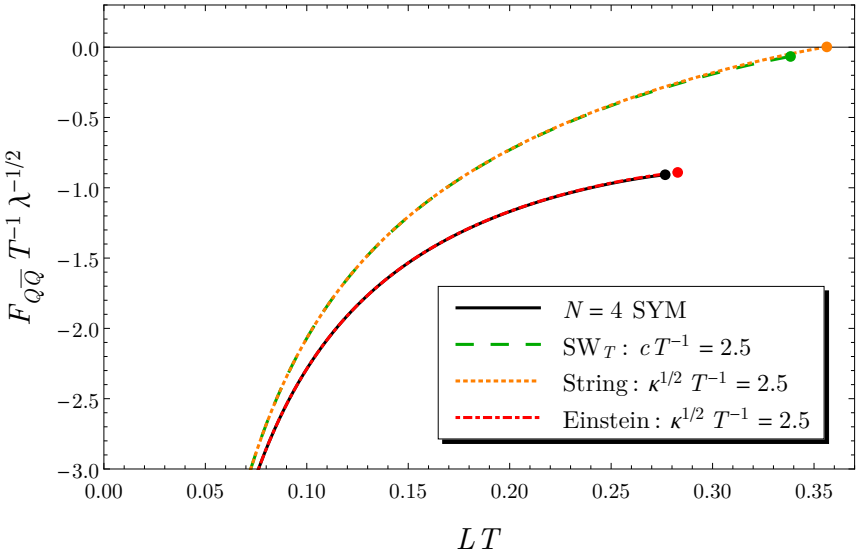

Figure 4. Free energy $F_{Q\bar{Q}}$ in $\mathcal{N} = 4$ SYM and in the non-conformal models at large dimensionless deformation-parameter-to-temperature ratios, c/T and $\sqrt{\kappa}/T$, respectively, for fixed temperature. To be able to discern details of the free energy close to the screening distance (marked by dots), we do not show the curves for very small distances. For small LT, all shown curves converge to one universal curve. All dimensionful quantities are measured in units of the temperature.

For quark separations L somewhat smaller than those shown in fig. 4, which we have left out of the plot to not obscure the details close to the screening distance (marked by the dots), the free energy approaches a single universal curve even for different models. That curve is given by the vacuum potential $V_{Q\bar{Q}}$ of $\mathcal{N} = 4$ SYM, see (4.6). This confirms our considerations concerning the small-distance behavior of $F_{Q\bar{Q}}$ in terms of the bulk picture in sec. 3.

Since the curves for all our models approach a single universal curve for small quark separation, we can sensibly compare the free energy in different theories.[5] In particular, let us compare the different non-conformal models to $\mathcal{N} = 4$ SYM. First we note that the 1-parameter Einstein-frame model is very robust against non-conformal deformation. The free energy in this model is only slightly above its value in $\mathcal{N} = 4$ SYM, even at the relatively large deformation considered here. On the other hand, in both the SW$_T$ and 1-parameter string-frame models the free energy increases well above its value in $\mathcal{N} = 4$ SYM upon introducing non-conformality. As a common property we observe that in all our models the free energy in the non-conformal models is above that in $\mathcal{N} = 4$ SYM. Hence $F_{Q\bar{Q}}$ in $\mathcal{N} = 4$ SYM appears to be a lower bound for estimating the free energy of a heavy quark–antiquark pair, if the latter is normalized such that for small distances it reduces to the potential at $T = 0$ given in (4.6). We expect this bound to apply to a large class of non-conformal holographic theories.

[5] *A priori*, the free energy is only defined up to an overall constant offset. However, by demanding that the free energy approaches the vacuum potential $V_{Q\bar{Q}}$ for small distances this ambiguity is fixed.

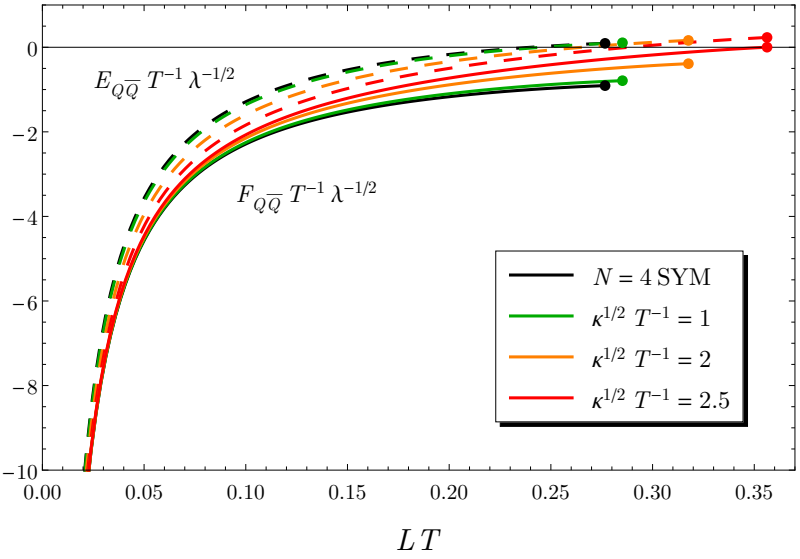

Figure 5. Free energy $F_{Q\bar{Q}}$ (solid curves) and binding energy $E_{Q\bar{Q}}$ (dashed curves) in $\mathcal{N} = 4$ SYM and the 1-parameter string-frame model at fixed temperature for varying deformation parameter. All dimensionful quantities are measured in units of the temperature.

Next, we compare the free energy $F_{Q\bar{Q}}$ and the binding energy $E_{Q\bar{Q}}$ in the 1-parameter string-frame model, as an example of a consistent non-conformal deformation of $\mathcal{N} = 4$ SYM. This will also allow us to check the statement we just made about the lower bound for the free energy at smaller values of the deformation. In fig. 5 we plot $F_{Q\bar{Q}}$ and $E_{Q\bar{Q}}$ in the 1-parameter string-frame model for varying dimensionless deformation parameter $\sqrt{\kappa}/T$. We see that in this model the free energy gradually increases with increasing deformation. Thus, it indeed always stays above its value in $\mathcal{N} = 4$ SYM, even for smaller deformations. The figure also shows that, as mentioned above, the free energy in different theories (corresponding to different values of the deformation) converges upon a single universal curve for small quark separations L.

We further observe in fig. 5 that, in contrast to the behavior of the free energy, the binding energy $E_{Q\bar{Q}}$ decreases with increasing deformation. Thus, the binding of the $Q\bar{Q}$ pair at a given L becomes stronger. (Recall that $E_{Q\bar{Q}}$ is actually the negative binding energy.) We have studied the behavior of the binding energy with respect to the deformation also in our other non-conformal models. We find that, as was the case for the free energy, the binding energy $E_{Q\bar{Q}}$, too, behaves very similarly in the SW_T model and in the 1-parameter string-frame model for which we have shown $E_{Q\bar{Q}}$ in fig. 5. Furthermore, this quantity is very robust in the 1-parameter Einstein-frame model, staying quantitatively close to its counterpart in $\mathcal{N} = 4$ SYM for all values of the deformation parameter. Also the feature that clearly distinguishes the two quantities $F_{Q\bar{Q}}$ and $E_{Q\bar{Q}}$ from each other turns out to be universal in all our non-conformal models: while $F_{Q\bar{Q}}(L)$ at fixed L increases with increasing non-conformality, $E_{Q\bar{Q}}(L)$ decreases with increasing non-conformality. $E_{Q\bar{Q}}(L)$ in $\mathcal{N} = 4$ SYM might possibly be an upper bound for the binding energy of a heavy

quark–antiquark pair in a large class of non-conformal theories.

6 Entropy and internal energy of a heavy quark pair

In this section we want to discuss two quantities that can be derived from the free energy $F_{Q\bar{Q}}$ of the heavy quark–antiquark pair, namely the entropy and the internal energy of the pair. For the derivation of these observables it is crucial to use the correct (temperature-independent) subtraction in the renormalization (3.6) of the free energy.

The entropy and the internal energy of the heavy quark–antiquark pair can be computed from the free energy using standard thermodynamic relations. In a given holographic model the heavy-quark free energy $F_{Q\bar{Q}}(L,T)$ depends on the inter-quark distance L and the temperature T of the medium. The entropy $S_{Q\bar{Q}}$ of the pair can be computed (following the definition also used in lattice QCD, see for example [61]) as the derivative

$$S_{Q\bar{Q}}(L,T) = -\frac{\partial F_{Q\bar{Q}}(L,T)}{\partial T}\,. \tag{6.1}$$

With the entropy in hand, the internal energy can be obtained from

$$U_{Q\bar{Q}}(L,T) = F_{Q\bar{Q}}(L,T) + TS_{Q\bar{Q}}(L,T)\,. \tag{6.2}$$

The explicit computation in our holographic models, where we have the parametric expressions (3.8) for $F_{Q\bar{Q}}$ and (2.11) for the distance L in terms of the bulk length scales z_t and z_h, is not entirely straightforward. We give details on the computation and an explicit formula for the derivative $\partial F_{Q\bar{Q}}/\partial T$ in appendix A.

Both the free and the internal energy are phenomenologically interesting as candidates for model potentials for the interaction of heavy quarks in a finite-temperature medium. Model potentials are used for the computation of properties of heavy quarkonia from Schrödinger-like equations in the spirit of potential non-relativistic QCD (pNRQCD; see [14] for a review, and *e. g.* [15] for more recent work including finite-temperature effects). At zero temperature, pNRQCD provides a systematic framework for the derivation of an effective $Q\bar{Q}$ potential. At non-zero temperature the choice of a potential to model the heavy-quark interaction is to some extent ambiguous. The internal and the free energy differ from each other due to the entropy contribution, and it is thus worth exploring the behavior of both of these quantities. See also, for instance, [62, 61, 63] for discussions of heavy-quark energies and potentials in the context of lattice QCD.

Let us first compute the $Q\bar{Q}$ entropy and internal energy in $\mathcal{N}=4$ SYM. The above formulae (6.1) and (6.2) can be evaluated explicitly based on the expressions (4.4) and (4.5) for $F_{Q\bar{Q}}(z_\mathrm{t})$ and $L(z_\mathrm{t})$, plugged into (A.4) in the appendix. We obtain the parametric expressions

$$\frac{S_{Q\bar{Q}}(z_\mathrm{t})}{\sqrt{\lambda}} = \frac{2\sqrt{\pi}\,\Gamma\left(\frac{3}{4}\right)}{\Gamma\left(\frac{1}{4}\right)}\,\frac{z_\mathrm{h}}{z_\mathrm{t}}\,\frac{5\left(1-\frac{z_\mathrm{t}^4}{z_\mathrm{h}^4}\right)f_\mathrm{a}^2 + \left[3\left(1-\frac{z_\mathrm{t}^4}{z_\mathrm{h}^4}\right)f_\mathrm{b} - 5f_\mathrm{a}\right]f_\mathrm{c}}{5\left(\frac{z_\mathrm{h}^4}{z_\mathrm{t}^4}-3\right)f_\mathrm{a} + 6\left(1-\frac{z_\mathrm{t}^4}{z_\mathrm{h}^4}\right)f_\mathrm{b}}\,, \tag{6.3}$$

and

$$\frac{U_{Q\bar{Q}}(z_t)}{\sqrt{\lambda}} = -\frac{5\,\Gamma\left(\frac{3}{4}\right)}{\sqrt{\pi}\,\Gamma\left(\frac{1}{4}\right)}\,\frac{1}{z_t}\,\frac{\left(1-\frac{z_t^4}{z_h^4}\right) f_a f_d}{5\left(1-3\frac{z_t^4}{z_h^4}\right) f_a + 6\frac{z_t^4}{z_h^4}\left(1-\frac{z_t^4}{z_h^4}\right) f_b}\,, \tag{6.4}$$

where f_a, f_b, f_c, and f_d depend on z_t^4/z_h^4: we define them as shorthand notation for the functions

$$f_a\left(\frac{z_t^4}{z_h^4}\right) = {}_2F_1\left(\frac{1}{2}, \frac{3}{4}; \frac{5}{4}; \frac{z_t^4}{z_h^4}\right)\,, \tag{6.5}$$

$$f_b\left(\frac{z_t^4}{z_h^4}\right) = {}_2F_1\left(\frac{3}{2}, \frac{7}{4}; \frac{9}{4}; \frac{z_t^4}{z_h^4}\right)\,, \tag{6.6}$$

$$f_c\left(\frac{z_t^4}{z_h^4}\right) = {}_2F_1\left(-\frac{1}{2}, -\frac{1}{4}; \frac{1}{4}; \frac{z_t^4}{z_h^4}\right)\,, \tag{6.7}$$

$$f_d\left(\frac{z_t^4}{z_h^4}\right) = {}_2F_1\left(-\frac{1}{2}, \frac{3}{4}; \frac{1}{4}; \frac{z_t^4}{z_h^4}\right)\,. \tag{6.8}$$

The entropy $S_{Q\bar{Q}}$ vanishes identically in the limit $T \to 0$, as can be verified analytically in $\mathcal{N} = 4$ SYM from formula (6.3). This implies that for $T = 0$ the internal energy coincides with the free energy. As we have seen before, in this case the free energy, and thus also the internal energy, is given by the zero-temperature potential $V_{Q\bar{Q}}$, see (4.6).

In fig. 6 we plot the internal energy $U_{Q\bar{Q}}$ and the free energy $F_{Q\bar{Q}}$ in $\mathcal{N} = 4$ SYM for increasing temperature (in AdS units set by $L_{\text{AdS}} = 1$) starting at $T = 0$. An inset shows the entropy $S_{Q\bar{Q}}$ for any $T > 0$ as a function of the dimensionless product LT. Note that in $\mathcal{N} = 4$ SYM, due to the absence of any further scales, the dimensionless entropy $S_{Q\bar{Q}}$ necessarily only depends on LT. The black solid curve in fig. 6 shows $V_{Q\bar{Q}}$.

At $T > 0$, the internal and free energies start to differ from each other and from their common $T = 0$ limit $V_{Q\bar{Q}}$ at intermediate L (compared to the screening distance, which in the figure is marked by a dot on the respective curve's endpoint). We have discussed the behavior of the free energy in secs. 4 and 5, so let us focus now on the entropy and the internal energy. As seen in the inset in fig. 6, the entropy increases monotonically with the quark separation L. A heuristic physical explanation of this observation might be that, as the size of the $Q\bar{Q}$ bound state increases, it has a growing overlap with the regime of the (thermal) length scales $L_{\text{th}} \sim 1/T$ of the surrounding medium. Therefore, the $Q\bar{Q}$ state can couple to an increasing number of modes of the medium, thus increasing its associated phase-space volume which leads to a rapid increase in entropy. With only the string configuration connecting the quark and the antiquark we cannot calculate the entropy of the pair for distances L larger than the screening distance L_s. When L is further increased above L_s one expects the entropy to grow until it eventually saturates at a value corresponding to the entropy of two single heavy quarks, $2S_Q$. We will calculate the latter in sec. 7 below. For $\mathcal{N} = 4$ SYM, for example, a comparison of $S_{Q\bar{Q}}$ in fig. 6 and S_Q in fig. 10 below shows that at L_s the entropy $S_{Q\bar{Q}}$ of the pair has reached about half the expected asymptotic value. In contrast to the free energy, the internal energy increases for fixed L upon increasing the temperature. It is always larger than the free energy due to the positive entropy contribution $TS_{Q\bar{Q}}(L) > 0$. Interestingly, the internal energy has

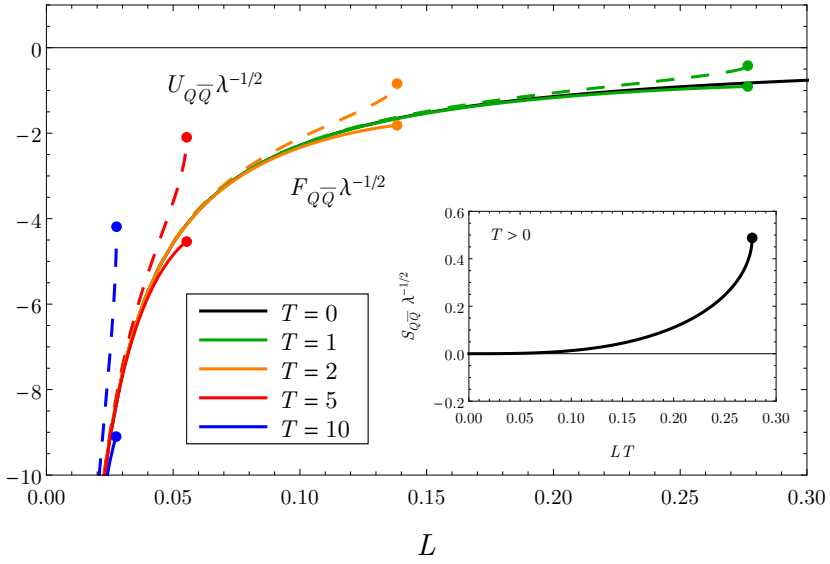

Figure 6. Internal energy $U_{Q\bar{Q}}(L)/\sqrt{\lambda}$ (dashed curves) and free energy $F_{Q\bar{Q}}(L)/\sqrt{\lambda}$ (solid curves) for varying temperature in $\mathcal{N} = 4$ SYM. The inset shows the entropy $S_{Q\bar{Q}}/\sqrt{\lambda}$ for an arbitrary fixed $T > 0$ as a function of LT. In the main plot, we express all dimensionful quantities in units specified by $L_{\text{AdS}} = 1$. The dots on the endpoints of the curves mark the screening distance. For very small L, the entropy approaches zero and both $U_{Q\bar{Q}}$ and $F_{Q\bar{Q}}$ approach a universal Coulombic curve given by (4.6).

an inflection point and curves upward close to the screening distance. Since the entropy approaches zero for small distances L, the internal energy approaches the free energy and shares with it the independence of T for small L.

Having gained an understanding of the behavior of the entropy and internal energy in $\mathcal{N} = 4$ SYM, next we investigate their behavior in our non-conformal models. Here, the entropy and subsequently the internal energy are computed numerically from the free energy. The qualitative dependence on temperature is similar to the one in $\mathcal{N} = 4$ SYM we discussed above. To study the impact of the deformation in more detail, in fig. 7 we show the internal energy as a function of the quark separation at fixed temperature in our non-conformal models for a large value of the dimensionless ratios of the deformation parameters and the temperature, $c/T = 2.5$ and $\sqrt{\kappa}/T = 2.5$ in the SW_T and 1-parameter models, respectively. In the inset, we plot the entropy as a function of LT using the same deformation parameters. For comparison, we also display the internal energy and entropy in $\mathcal{N} = 4$ SYM (black curves). We see that the entropy behaves similarly as in $\mathcal{N} = 4$ SYM discussed above, *cf.* the inset in fig. 6. While $S_{Q\bar{Q}}$ vanishes for $L = 0$, it increases monotonically for increasing L towards its maximum at the screening distance. The internal energy $U_{Q\bar{Q}}(L)$ in the non-conformal models has a shape similar to that in $\mathcal{N} = 4$ SYM. In particular, its slope increases towards the screening distance L_{s}, too, which can be traced back to the strong increase of $S_{Q\bar{Q}}$ towards L_{s}.

For small distances L, the behavior of the internal energy is dominated by that of the free energy because the entropy approaches zero in all our models. Accordingly, like

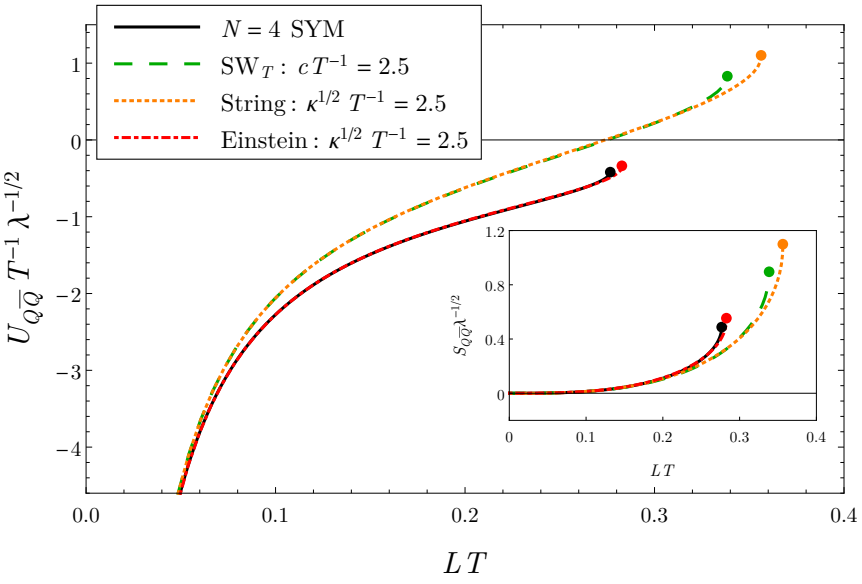

Figure 7. Internal energy $U_{Q\bar{Q}}(L)/(T\sqrt{\lambda})$ at fixed temperature in $\mathcal{N}=4$ SYM and non-conformal models at large deformations with $c/T = 2.5$ and $= \sqrt{\kappa}/T = 2.5$ for the SW_T and 1-parameter models, respectively. The inset shows the entropy $S_{Q\bar{Q}}/\sqrt{\lambda}$ as a function of LT. For very small L, the entropy approaches zero in all models and $U_{Q\bar{Q}}$ in all models converges to a universal Coulombic curve.

the free energy discussed in sec. 5, also the internal energy in all non-conformal models converges to one universal curve for small L, namely the one in $\mathcal{N}=4$ SYM given by the zero-temperature potential $V_{Q\bar{Q}}$ in (4.6).

Differences between the behavior of the internal energy in our non-conformal models and the behavior in $\mathcal{N}=4$ SYM generally appear at intermediate and large L. In all of our non-conformal models the entropy at fixed distance decreases relative to its value in $\mathcal{N}=4$ SYM for the chosen degree of non-conformality (and the same holds for smaller values of the non-conformality parameter, see below). In the overall effect on the internal energy, however, the increase in the free energy that we have seen in sec. 5 overwhelms the decrease in the entropy in $U_{Q\bar{Q}} = F_{Q\bar{Q}} + TS_{Q\bar{Q}}$, such that the internal energy in our non-conformal models is larger than in $\mathcal{N}=4$ SYM. This indicates that $U_{Q\bar{Q}}$ in $\mathcal{N}=4$ SYM might possibly constitute a lower bound on the internal energy for a large class of non-conformal theories. Looking at the different non-conformal models in more detail, we find that the 1-parameter Einstein-frame model is very robust against non-conformal deformation, and both $S_{Q\bar{Q}}$ and $U_{Q\bar{Q}}$ stay very close to their respective values in $\mathcal{N}=4$ SYM for all distances L. The effect of the non-conformality is larger and again similar in the SW_T and 1-parameter models.

To not clutter the presentation, we have refrained in fig. 7 from also showing the free energy. To gain a better understanding of the relative behavior of the free and the internal energy in a non-conformal model, we now focus on the 1-parameter string-frame model as an example of a consistent deformation of AdS_5-Schwarzschild. Moreover, in this

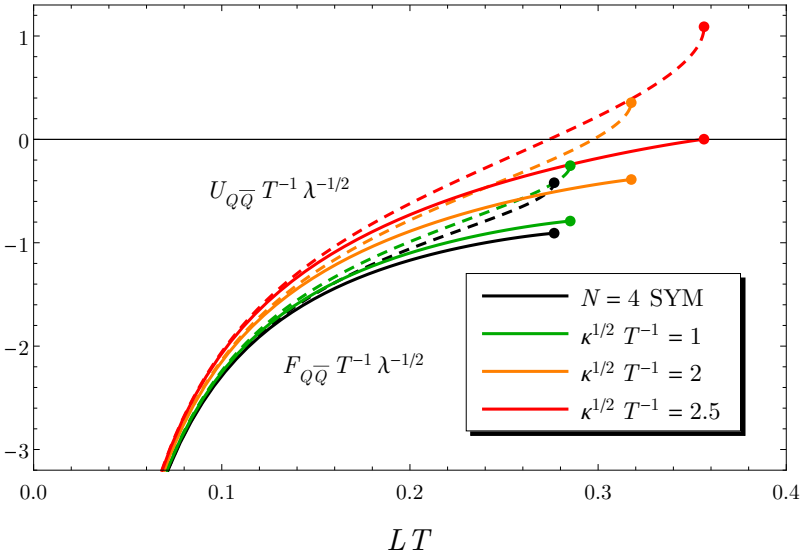

Figure 8. Internal energy $U_{Q\bar{Q}}(L)/(T\sqrt{\lambda})$ (dashed curves) and free energy $F_{Q\bar{Q}}(L)/(T\sqrt{\lambda})$ (solid curves) at fixed temperature in $\mathcal{N} = 4$ SYM (black curves) and the 1-parameter string-frame model for varying deformation parameter. For very small L, both $U_{Q\bar{Q}}$ and $F_{Q\bar{Q}}$ approach a universal Coulombic curve.

way we can check whether the internal energy in the deformed model is larger than the corresponding internal energy in $\mathcal{N} = 4$ SYM also for smaller values of the deformation. In fig. 8 we show the dependence of the internal energy and free energy on the deformation parameter in the 1-parameter string-frame model, starting from the undeformed theory, *i. e.* $\mathcal{N} = 4$ SYM (black curves). Like the free energy, the internal energy increases with increasing deformation parameter, and indeed is larger than in $\mathcal{N} = 4$ SYM for all choices of the deformation parameter. As in $\mathcal{N} = 4$ SYM, also in the non-conformal model the internal energy approaches the free energy for small quark separation L.

We have performed a similar analysis for the other non-conformal models. We observe that the change of the internal energy with respect to $\mathcal{N} = 4$ SYM induced by non-conformality is positive. In the 1-parameter Einstein-frame model it is particularly small while it is larger and similar in the SW_T model and in the 1-parameter string-frame model. As the entropy approaches zero for small L in all our non-conformal models, *cf.* the inset in fig. 7, we find that at small quark separations, $F_{Q\bar{Q}}$ and $U_{Q\bar{Q}}$ in all theories approach as a common limit the free energy in $\mathcal{N} = 4$ SYM, which in turn approaches the zero-temperature potential $V_{Q\bar{Q}}$ for small L. Thus, in all of our models the internal and free energy differ only for intermediate and large quark separations. A similar behavior is also observed in lattice simulations [61].

7 Free energy, entropy, and internal energy of a single heavy quark

In the derivation of the holographic formula for the $Q\bar{Q}$ free energy in sec. 3, we have obtained as a by-product the definition (3.14) of the free energy of a single quark in the

hot medium described by our holographic models. In this section, we will put that relation to use and compute the free energy of a single heavy 'test' quark. We will also study the entropy and internal energy associated with the free energy. An analysis of these single-quark quantities in our class of non-conformal models, with a focus on the impact of non-conformal deformations of $\mathcal{N} = 4$ SYM, has not been performed in the literature so far.[6]

We have defined the free energy F_Q in (3.14), and define the corresponding entropy and internal energy by standard thermodynamic relations,

$$S_Q = -\frac{\partial F_Q}{\partial T}\,, \tag{7.1}$$

$$U_Q = F_Q + T S_Q\,. \tag{7.2}$$

Let us start with $\mathcal{N} = 4$ SYM. In this case, the expression (3.14) can easily be evaluated explicitly, using the AdS-Schwarzschild metric (4.1). We obtain for the single-quark free energy, entropy, and internal energy

$$F_Q = -\frac{\sqrt{\lambda}}{2}\,T\,, \qquad S_Q = \frac{\sqrt{\lambda}}{2}\,, \qquad U_Q = 0\,. \tag{7.3}$$

These values have also been obtained in [66]. Since $\mathcal{N} = 4$ SYM is a conformal theory, at $T > 0$ only the temperature itself is available as a dimensionful quantity for the problem at hand. Thus, the relation $F_Q \propto T$ already follows from dimensional analysis. The non-analytic square-root dependence on the 't Hooft coupling is, however, a non-trivial outcome of the computation. Interestingly, the free energy is entirely determined by the entropic contribution, and the internal energy vanishes.

We can analytically compute the above quantities also in the SW_T model and the 1-parameter Einstein-frame model. Let us start with the SW_T model. Due to the simple relation of the temperature and the horizon position, $z_\mathrm{h} = 1/(\pi T)$, we can explicitly express F_Q as a function of T and compute the entropy and internal energy. We find

$$F_Q = -\frac{\sqrt{\lambda}}{2\pi}\exp\left(\frac{c^2}{\pi^2 T^2}\right)\left[\pi T - 2c\,\mathcal{F}\left(\frac{c}{\pi T}\right)\right]\,, \tag{7.4}$$

$$S_Q = \frac{\sqrt{\lambda}}{2}\exp\left(\frac{c^2}{\pi^2 T^2}\right)\,, \tag{7.5}$$

$$U_Q = \frac{\sqrt{\lambda}}{2\sqrt{\pi}}\,c\,\mathrm{erfi}\left(\frac{c}{\pi T}\right)\,, \tag{7.6}$$

where $\mathcal{F}$ is the Dawson integral and erfi the 'imaginary' error function defined by $\mathrm{erfi}(x) = -\mathrm{i}\,\mathrm{erf}(\mathrm{i}x)$.[7] We recall that λ denotes the bulk quantity defined by $\sqrt{\lambda} = L^2_\mathrm{AdS}/\alpha'$ and is

[6] Previous work with different focus includes [26] which studies the single-quark free energy in a bottom-up framework tuned to model Yang–Mills thermodynamics, and the recent works [64, 65]. For a general discussion of single-quark thermodynamics in holographic models see [66].

[7] The Dawson integral is defined by

$$\mathcal{F}(x) = \mathrm{e}^{-x^2}\int_0^x \mathrm{d}y\,\mathrm{e}^{y^2}\,,$$

a proxy for the coupling strength in the boundary theory, *cf.* (2.12) and the discussion thereof. As we will see explicitly below, for high temperatures F_Q, S_Q, and U_Q approach their values in $\mathcal{N}=4$ SYM from above. However, as T is lowered they significantly increase above the conformal values.

In the 1-parameter Einstein-frame model, we can only find closed-form expressions for F_Q, S_Q, and U_Q as functions of z_h, since we cannot analytically invert the temperature function $T(z_\mathrm{h})$ in (5.7). We find

$$F_Q(z_\mathrm{h}) = -\frac{\sqrt{\lambda}}{8\sqrt{2}\pi}\sqrt{\kappa}\left[4\,\Gamma\left(\frac{3}{4}\right)+\gamma\left(-\frac{1}{4},\frac{\kappa^2 z_\mathrm{h}^4}{4}\right)\right], \tag{7.7}$$

$$S_Q(z_\mathrm{h}) = \frac{2\sqrt{\lambda}}{3}\,\frac{1}{\kappa^2 z_\mathrm{h}^4}\,\frac{\exp\left(-\frac{1}{2}\kappa^2 z_\mathrm{h}^4\right)\left[\exp\left(\frac{1}{4}\kappa^2 z_\mathrm{h}^4\right)-1\right]^2}{1-\exp\left(\frac{1}{4}\kappa^2 z_\mathrm{h}^4\right)+\frac{1}{3}\kappa^2 z_\mathrm{h}^4}, \tag{7.8}$$

$$U_Q(z_\mathrm{h}) = \frac{\sqrt{\lambda}}{6\pi}\left\{\frac{1}{z_\mathrm{h}}\,\frac{1-\exp\left(-\frac{1}{4}\kappa^2 z_\mathrm{h}^4\right)}{1-\exp\left(\frac{1}{4}\kappa^2 z_\mathrm{h}^4\right)+\frac{1}{3}\kappa^2 z_\mathrm{h}^4}-\frac{3\sqrt{2}}{8}\sqrt{\kappa}\left[4\,\Gamma\left(\frac{3}{4}\right)+\gamma\left(-\frac{1}{4},\frac{\kappa^2 z_\mathrm{h}^4}{4}\right)\right]\right\}, \tag{7.9}$$

where γ is the incomplete Γ-function.[8] Although we are not able to express these quantities symbolically in terms of the temperature T, it is straightforward to analyze their behavior numerically.

For the 1-parameter string-frame model, the additional terms in the warp factors prohibit a solution of the integrals for F_Q, S_Q, and U_Q in closed form. Nevertheless, we can numerically evaluate the definition (3.14) for the free energy and easily compute the entropy and internal energy from it.

When we consider a single heavy quark there is no intrinsic length scale in the problem, and as a consequence we cannot express our results in terms of a dimensionless quantity similar to LT that we used in the case of the quark–antiquark pair before. Instead, the results will depend on the temperature in each of the different models. In order to sensibly compare temperatures in these different theories we choose, among various possibilities, the following procedure which was discussed for example in [68] in the context a specific holographic model [69]. We consider the dimensionless trace of the energy–momentum tensor, $(\epsilon-3p)/T^4$, which was calculated in [58] for our non-conformal models. It turns out to have a pronounced maximum, the position of which is a function of the respective deformation parameter. At temperatures above the position of the maximum, the behavior of $(\epsilon-3p)/T^4$ strongly resembles that found above T_c in lattice studies of QCD, for example in [56, 70, 68]. We therefore identify the position of the maximum found in our models

and the error function by

$$\mathrm{erf}(x) = \frac{2}{\sqrt{\pi}}\int_0^x \mathrm{d}t\,\mathrm{e}^{-t^2},$$

see [67]. The latter is related to the Dawson integral by $\mathcal{F}(x) = -\mathrm{i}\sqrt{\pi}\mathrm{e}^{-x^2}\,\mathrm{erf}(\mathrm{i}x)/2$.

[8] The incomplete Γ-function is defined by

$$\gamma(a,x) = \int_x^\infty \mathrm{d}t\,t^{a-1}\mathrm{e}^{-t},$$

see [67]. It is related to the ordinary Γ-function by $\gamma(a,0)=\Gamma(a)$.

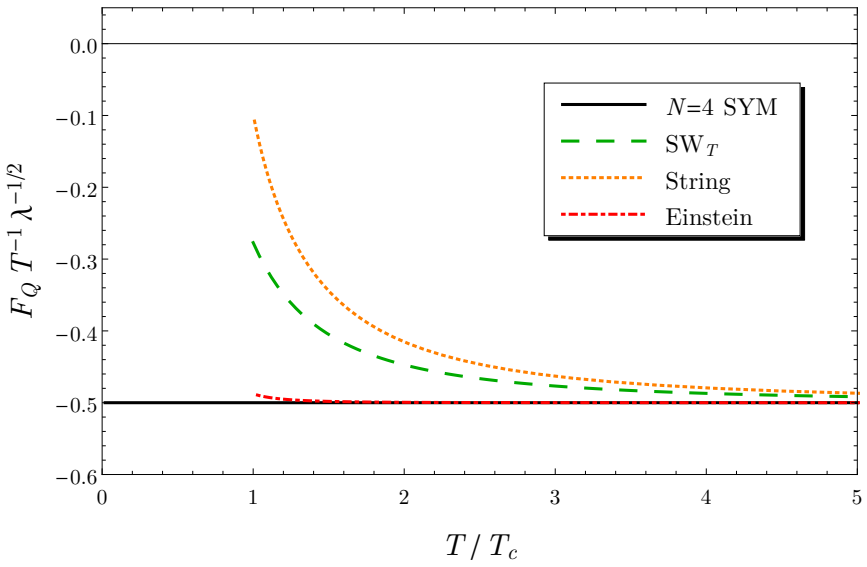

Figure 9. Single-quark free energy as a function of temperature in $\mathcal{N} = 4$ SYM and our non-conformal models. We have scaled out the dominant T-dependence of F_Q. The scale T_c is explained in the text.

with T_c [58], which gives $T_c/c \approx 0.494$ and $T_c/\sqrt{\kappa} \approx 0.394$ in the SW$_T$ model and in the 1-parameter models, respectively. For definiteness, we assume $T_c = 176\,\text{MeV}$ to introduce physical units, but the choice of this particular value will not be relevant for our results.[9] We emphasize that our non-conformal models do not exhibit an actual phase transition and hence do not have a 'critical temperature'. The models are expected to resemble the high-temperature (deconfined) phase of QCD. With the procedure just described we only fix the temperature range in which our models should be compared to QCD, $T \geq T_c$. Accordingly, we will show our observables only in this range. Finally, in $\mathcal{N} = 4$ SYM the trace of the energy–momentum tensor vanishes identically for all temperatures, so that there is no analogous way to define T_c. Thus, the choice $T_c = 176\,\text{MeV}$ is completely arbitrary in this case. In the following, we scale F_Q, S_Q, and U_Q such that the dependence on T becomes trivial for $\mathcal{N} = 4$ SYM.

We plot the free energy, entropy and internal energy of the heavy quark as functions of the temperature in $\mathcal{N} = 4$ SYM and in all our non-conformal models in figs. 9, 10, and 11, respectively. We have seen in several observables before that the 1-parameter Einstein-frame model is very robust and stays quantitatively close to $\mathcal{N} = 4$ SYM. The quantities F_Q, S_Q, and U_Q are no exception and are very close to their respective values in $\mathcal{N} = 4$ SYM for almost all T, as seen in the three figures. All three quantities exhibit

[9] Various other methods to compare the temperatures of different theories or to fix the parameters of a holographic theory for comparison to QCD have been discussed in the literature, see [30, 31, 71] for some examples. The values for the deformation parameters that we obtain from fixing the position of the maximum in $(\epsilon - 3p)/T^4$ to a particular value of T_c are in the same ballpark as those obtained with other methods, see for instance [30, 31]. We would like to point out that the qualitative conclusions below do not change if we vary the deformation parameters around the values given here.

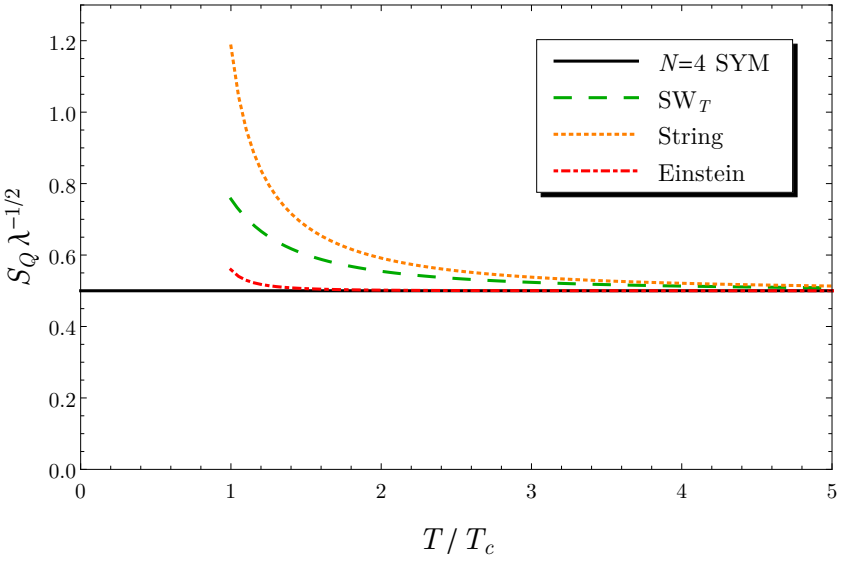

Figure 10. Single-quark entropy as a function of temperature in $\mathcal{N} = 4$ SYM and our non-conformal models. The scale T_c is explained in the text.

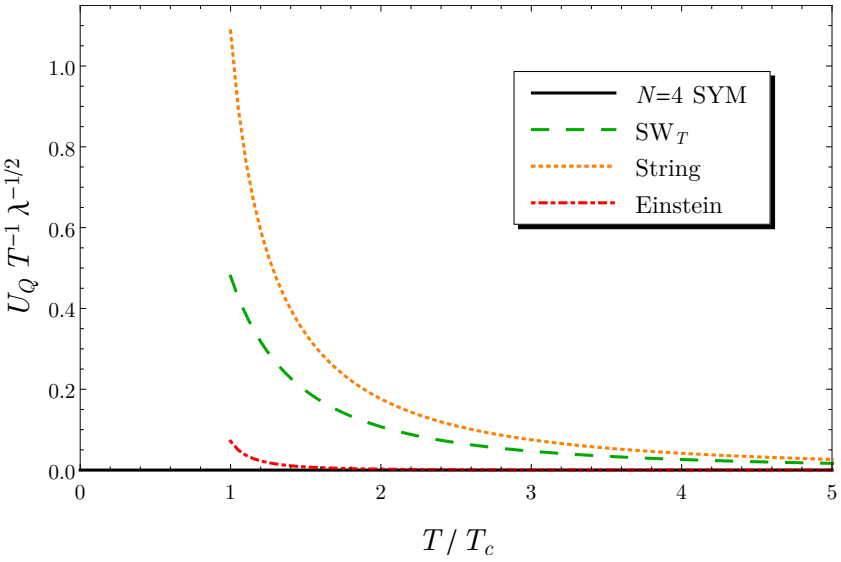

Figure 11. Single-quark internal energy as a function of temperature in $\mathcal{N} = 4$ SYM and our non-conformal models. We have scaled out a factor of T. The scale T_c is explained in the text. Note that the internal energy vanishes identically in $\mathcal{N} = 4$ SYM.

a stronger dependence on the temperature in both the SW$_T$ model and the 1-parameter string-frame model. The latter deviates farthest from the behavior seen in $\mathcal{N} = 4$ SYM. For large temperatures, F_Q, S_Q, and U_Q approach their values in $\mathcal{N} = 4$ SYM from above. This implies an interesting universal behavior. In all of our non-conformal models, F_Q, S_Q, and U_Q are larger than their respective values in $\mathcal{N} = 4$ SYM for all temperatures. Even choosing a different procedure to normalize the temperature scale in each model would not

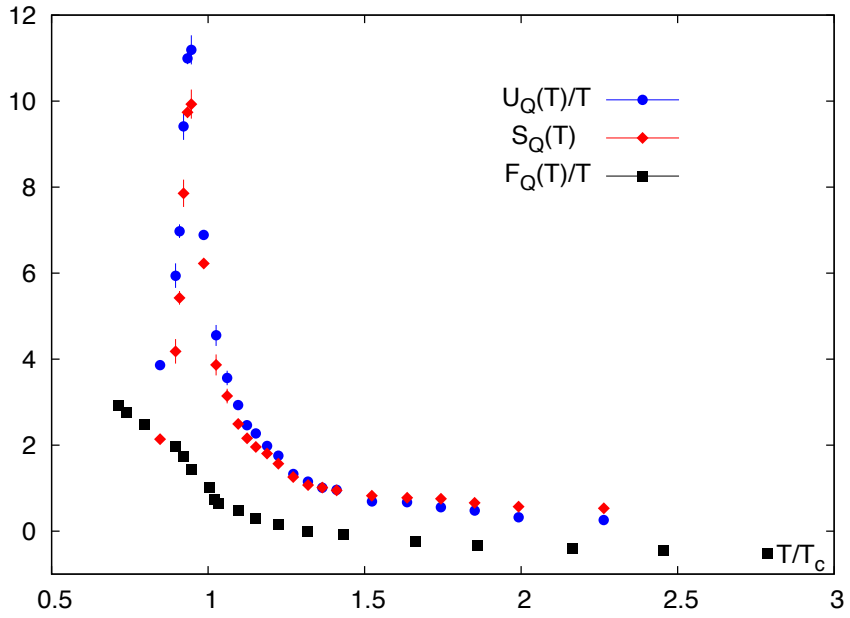

Figure 12. Free energy over temperature (F_Q/T, black squares), entropy (S_Q, red diamonds), and internal energy over temperature (U_Q/T, blue circles) of a heavy quark obtained from a 2+1-flavor lattice QCD calculation [55].

change this finding. It appears likely that this observation holds in a large class of theories.

Computations of the single-quark free energy in lattice QCD have been performed for instance in [17, 18, 61, 55, 72, 73]. In these studies, the single-quark free energy is defined in terms of the large-distance behavior of the expectation value of a Polyakov loop correlator. The latter yields the free energy of a heavy $Q\bar{Q}$ pair at large quark separation, where the $Q\bar{Q}$ free energy in fact approaches a constant value F_∞. At least in the deconfined phase where the far-separated quarks are screened from each other, one can interpret that free energy as twice the single-quark free energy, $F_\infty = 2F_Q$. In a similar way, lattice results have been obtained for the entropy S_Q and the internal energy U_Q of a single heavy quark. In the following, for concreteness, we will compare to 2+1-flavor lattice QCD results from [55]. The qualitative behavior that we are going to compare to is similar in the other lattice studies cited above.[10] The data for F_Q/T, S_Q and U_Q/T from [55] are shown in fig. 12. For this figure we made use of the freedom to add a constant to F_Q and U_Q, and we have chosen this constant as $-0.6\,T_c$ relative to the data shown in [55].

In the case of the single heavy quark the comparison of our holographic to the lattice results is not completely straightforward. As we have seen, in the non-conformal models F_Q, S_Q and U_Q exhibit a universal rise above their values in $\mathcal{N} = 4$ SYM, but their size strongly depends on the chosen non-conformal model, and for each model on the choice

[10] The recent study [73] with 2+1 dynamical flavors with physical masses finds deviations from previous calculations, most clearly visible in a less steeply falling entropy S_Q around T_c. These deviations may be attributed to quark mass dependences and the lack of a continuum extrapolation in previous results. On the level of the comparison with our generic holographic models, however, this difference is of minor relevance.

of the deformation parameter. Further, the free energy and the internal energy are only defined up to an arbitrary constant shift. This freedom could be fixed for the case of a $Q\bar{Q}$ pair by fixing the small-distance limit of the free energy $F_{Q\bar{Q}}$ to the vacuum potential $V_{Q\bar{Q}}$ of $\mathcal{N}=4$ SYM, see sec. 5. There is no analogue of such a condition in the case of a single quark. Finally, in all our models the results for all three quantities are proportional to $\sqrt{\lambda}$. As we have discussed at the end of sec. 2, especially for the non-conformal models λ should be considered as a free parameter of the model, and it can even be different for different values of the non-conformal deformation parameter. In view of these caveats, we restrict the comparison with the lattice results to some qualitative features. Further detailed study in concrete models is needed to obtain a more complete picture of this comparison. Obviously, we again concentrate on the region $T \geq T_c$ as our holographic models are expected to apply to the deconfined phase only.

The free energy in units of temperature F_Q/T from [55] is represented by the black squares in fig. 12. Closely above T_c we observe a decrease of F_Q/T which flattens above about $1.3\,T_c$ and approaches a constant.[11] The free energy in our non-conformal holographic models exhibits a similar behavior above T_c, as we can see in fig. 9 which also shows the ratio F_Q/T. Note that F_Q/T is a constant in $\mathcal{N}=4$ SYM. Hence the non-conformality is crucial for obtaining an F_Q/T that resembles data from lattice QCD.

The lattice data for S_Q are shown as red diamonds in fig. 12. S_Q from the lattice is peaked at $T=T_c$. The entropy is a T-independent constant in $\mathcal{N}=4$ SYM, again illustrating the need to introduce non-conformality to model QCD physics at $T \gtrsim T_c$. Indeed, in our non-conformal models we find an increase of S_Q as T is lowered towards T_c, qualitatively similar to the lattice results, see fig. 10. A heuristic explanation for the decrease of the entropy with temperature above T_c might be as follows. As the temperature increases, the screening length in the medium decreases and the quark interacts with a smaller volume around it. Thus, its phase space and, accordingly, its entropy decreases (*cf.* a related discussion in [18]).

The lattice data for U_Q/T are shown as the filled blue circles in fig. 12. As in the case of S_Q, they exhibit a strong peak at $T=T_c$ and a subsequent decrease and flattening. A similar behavior of U_Q/T is found in our non-conformal models, see fig. 11. Again, the $\mathcal{N}=4$ SYM result does not show such a behavior.

In summary, our comparison of the single-quark free energy, entropy and internal energy shows an agreement of at least some main properties of these quantities in the deconfined region $T \geq T_c$ relevant for the application of our holographic models. In particular, we observe that it is necessary to introduce non-conformality in the holographic model in order to achieve similarity to the lattice results.

[11] In [73] it is observed that this quantity rises again at very high temperatures. This can be attributed to the perturbative running of the strong coupling constant. We thus should not expect to see this effect in a holographic model that is asymptotically AdS in the UV.

8 Summary and conclusions

The free energy of a heavy quark–antiquark pair in a thermal medium provides important information about the medium and its interaction with color sources. In this paper we have reconsidered the calculation of the free energy of the static pair in the framework of the AdS/CFT correspondence, where it is related to the action of a macroscopic string connecting the quark and the antiquark and hanging down into the holographic dimension. We have argued that the UV renormalization required for this action should not introduce a temperature dependence. With this condition, a consistent picture for the behavior of the free energy emerges. Applying a temperature-independent renormalization procedure we in fact find the free energy from AdS/CFT to be in qualitative agreement with data from lattice gauge theory. We observe that a temperature-dependent renormalization procedure widely used in the literature gives rise to the (negative) binding energy of the pair rather than to its free energy. As we have shown, the free energy and the binding energy have a markedly different dependence on temperature. We have then computed the entropy and the internal energy of the static quark–antiquark pair in the medium from the free energy and have discussed their properties. In order to obtain these observables it is essential to have the correct temperature dependence of the free energy. Finally, we have also computed the free energy, the entropy and the internal energy of a single heavy quark in the thermal medium, and have compared their behavior to that obtained in lattice gauge theory.

We have performed these calculations in several holographic theories, starting with pure AdS_5 space dual to $\mathcal{N} = 4$ SYM. We have also considered deformed AdS-type spaces holographically dual to non-conformal deformations of $\mathcal{N} = 4$ SYM. The latter theories are expected to share more properties with the actual quark–gluon plasma studied in heavy ion collisions than does conformal $\mathcal{N} = 4$ SYM. Our aim in the present paper was explicitly not to investigate a particular holographic model for QCD. Instead, we have examined several classes of non-conformal models and have looked for universal behavior of our observables under non-conformal deformations. We have indeed found hints that, for any given distance, the free energy $F_{Q\bar{Q}}$ and the internal energy $U_{Q\bar{Q}}$ of a static quark pair in our non-conformal theories are consistently larger than their respective values in $\mathcal{N} = 4$ SYM. The binding energy $E_{Q\bar{Q}}$, on the other hand, consistently decreases with respect to its value in $\mathcal{N} = 4$ SYM under non-conformal deformation. We expect similar bounds to hold in larger classes of holographic theories. Also the free energy, entropy and the internal energy of single heavy quarks show a universal behavior under non-conformal deformations, being consistently larger than the respective $\mathcal{N} = 4$ SYM values. For these single-quark observables, a non-conformality is even necessary in order to obtain a non-trivial behavior.

Our considerations concerning the renormalization of the temporal Wegner–Wilson loop and the corresponding temperature dependence in holographic theories are very general. Here we have studied the effects of a temperature-independent renormalization procedure only for simple classes of holographic theories. It would obviously be interesting to extend these investigations to more complex plasmas, for example with chemical potential, and to more sophisticated holographic models for the actual quark–gluon plasma.

The question how heavy quarkonia behave in the quark–gluon plasma is highly relevant

for phenomenology, but difficult to answer for theory. We hope that the holographic calculation of the free energy, entropy and internal energy of a static quark pair in a strongly coupled medium can give some useful input in this context. In particular, the holographic results could be helpful for constructing the potential to be used in the Schrödinger equation describing heavy quarkonia in the medium. Also the discussion whether the dissociation of heavy quarkonia in the quark–gluon plasma is due to an entropic force (see for example [74, 75]) might benefit from our results concerning the temperature dependence of the entropy and internal energy of the pair at strong coupling.

Acknowledgments

We would like to thank S. Gubser, J. Pawlowski, A. Rothkopf, and S. Theisen for helpful discussions. A. S. acknowledges support in the framework of the cooperation contract between the GSI Helmholtzzentrum für Schwerionenforschung and Heidelberg University.

A Computation of the entropy of a heavy quark pair

Here we give details on the computation of the $Q\bar{Q}$ entropy $S_{Q\bar{Q}}$ discussed in sec. 6.

We use the basic thermodynamic formula $S_{Q\bar{Q}} = -\partial F_{Q\bar{Q}}/\partial T$ where it is understood that the inter-quark distance L is to be kept constant. An implementation of this formula is not entirely straightforward. The issue that arises is that the free energy $F_{Q\bar{Q}}$, as well as the distance L, are only known as integrals in terms of the bulk length scales z_t and z_h, see (3.8) and (2.11), respectively. Therefore, while these integrals can be readily computed numerically (or even analytically for $\mathcal{N} = 4$ SYM), the differentiation with respect to the temperature T while keeping the distance L constant is more involved.

In the following we use a notation in which a vertical bar with a subscripted variable indicates that this variable is kept constant. We will suppress any dependence on a possible deformation parameter. If present in the model under consideration, the deformation parameter is always assumed to be kept constant.

We first note that in $\mathcal{N} = 4$ SYM and in the SW_T model the relation between z_t and T is one-to-one, namely $T = 1/(\pi z_\mathrm{h})$. For the consistently deformed 1-parameter models this relation is modified but indeed remains one-to-one in the parameter range we consider in this paper, $0 \leq \sqrt{\kappa}/T \leq 2.5$. The relation ceases to be one-to-one only for $\sqrt{\kappa}/T > 2.94$, see also footnote 4. It is therefore straightforward to obtain $z_\mathrm{h} = z_\mathrm{h}(T)$ for all our models.

We further recall from sec. 2 that for a given inter-quark distance L smaller than the screening distance L_s there are two different string solutions connecting the quark and the antiquark, with the one staying further away from the horizon z_h being energetically favored. Hence for $0 \leq L \leq L_\mathrm{s}$ there are two branches of solutions, of which we consider mainly the energetically favored branch in this paper. In this branch L monotonically increases with increasing z_t, while in the branch with the energetically disfavored configurations L monotonically decreases with increasing z_t. Treating each of the branches separately, we can therefore invert $L(z_\mathrm{t}, T)$ to obtain $z_\mathrm{t} = z_\mathrm{t}(L, T)$.

As a consequence of these considerations we can write

$$\left.\frac{\partial F_{Q\bar{Q}}(z_\mathrm{t},z_\mathrm{h})}{\partial T}\right|_L = \left.\frac{\partial F_{Q\bar{Q}}}{\partial z_\mathrm{h}}\right|_{z_\mathrm{t}} \frac{\partial z_\mathrm{h}}{\partial T} + \left.\frac{\partial F_{Q\bar{Q}}}{\partial z_\mathrm{t}}\right|_{z_\mathrm{h}} \left.\frac{\partial z_\mathrm{t}}{\partial T}\right|_L , \tag{A.1}$$

where on $\partial z_\mathrm{h}/\partial T$ we may omit the specification of the variable that is to be kept constant because z_h is actually a function of T only. Next, we have to evaluate $\partial z_\mathrm{t}/\partial T$ with L kept constant. Using

$$0 \stackrel{!}{=} \mathrm{d}L = \left.\frac{\partial L}{\partial z_\mathrm{t}}\right|_{z_\mathrm{h}} \mathrm{d}z_\mathrm{t} + \left.\frac{\partial L}{\partial z_\mathrm{h}}\right|_{z_\mathrm{t}} \mathrm{d}z_\mathrm{h} = \left.\frac{\partial L}{\partial z_\mathrm{t}}\right|_{z_\mathrm{h}} \mathrm{d}z_\mathrm{t} + \left.\frac{\partial L}{\partial z_\mathrm{h}}\right|_{z_\mathrm{t}} \frac{\partial z_\mathrm{h}}{\partial T}\,\mathrm{d}T , \tag{A.2}$$

we derive

$$\left.\frac{\partial z_\mathrm{t}}{\partial T}\right|_L = -\left(\left.\frac{\partial L}{\partial z_\mathrm{t}}\right|_{z_\mathrm{h}}\right)^{-1} \left.\frac{\partial L}{\partial z_\mathrm{h}}\right|_{z_\mathrm{t}} \frac{\partial z_\mathrm{h}}{\partial T} . \tag{A.3}$$

Finally, we obtain

$$S_{Q\bar{Q}} = -\left.\frac{\partial F_{Q\bar{Q}}(z_\mathrm{t},z_\mathrm{h})}{\partial T}\right|_L = -\left(\left.\frac{\partial F_{Q\bar{Q}}}{\partial z_\mathrm{h}}\right|_{z_\mathrm{t}} - \left.\frac{\partial F_{Q\bar{Q}}}{\partial z_\mathrm{t}}\right|_{z_\mathrm{h}} \frac{\left.\frac{\partial L}{\partial z_\mathrm{h}}\right|_{z_\mathrm{t}}}{\left.\frac{\partial L}{\partial z_\mathrm{t}}\right|_{z_\mathrm{h}}}\right) \frac{\partial z_\mathrm{h}}{\partial T} , \tag{A.4}$$

which can be directly implemented on the basis of the numerical routines (or analytic expressions) for $F_{Q\bar{Q}} = F_{Q\bar{Q}}(z_\mathrm{t}, z_\mathrm{h})$ and $L = L(z_\mathrm{t}, z_\mathrm{h})$.

References

[1] J. M. Maldacena, *The Large-N limit of superconformal field theories and supergravity*, *Adv. Theor. Math. Phys.* **2** (1998) 231 [hep-th/9711200].

[2] S. S. Gubser, I. R. Klebanov, and A. M. Polyakov, *Gauge theory correlators from noncritical string theory*, *Phys. Lett.* **B428** (1998) 105 [hep-th/9802109].

[3] E. Witten, *Anti-de Sitter space and holography*, *Adv. Theor. Math. Phys.* **2** (1998) 253 [hep-th/9802150].

[4] J. Casalderrey-Solana, H. Liu, D. Mateos, K. Rajagopal, and U. A. Wiedemann, *Gauge/String Duality, Hot QCD and Heavy Ion Collisions*, Cambridge Univ. Pr., 2014.

[5] O. DeWolfe, S. S. Gubser, C. Rosen, and D. Teaney, *Heavy ions and string theory*, *Prog. Part. Nucl. Phys.* **75** (2014) 86 [arXiv:1304.7794].

[6] I. Arsene *et al.* [BRAHMS Collaboration], *Quark-gluon plasma and color glass condensate at RHIC? The perspective from the BRAHMS experiment*, *Nucl. Phys.* **A757** (2005) [nucl-ex/0410020].

[7] B. B. Back *et al.* [PHOBOS Collaboration], *The PHOBOS perspective on discoveries at RHIC*, *Nucl. Phys.* **A757** (2005) 28 [nucl-ex/0410022].

[8] J. Adams *et al.* [STAR Collaboration], *Experimental and theoretical challenges in the search for the quark gluon plasma: The STAR collaboration's critical assessment of the evidence from RHIC collisions*, *Nucl. Phys.* **A757** (2005) 102 [nucl-ex/0501009].

[9] K. Adcox *et al.* [PHENIX Collaboration], *Formation of dense partonic matter in relativistic nucleus nucleus collisions at RHIC: Experimental evaluation by the PHENIX collaboration*, *Nucl. Phys.* **A757** (2005) 184 [nucl-ex/0410003].

[10] K. Aamodt *et al.* [ALICE Collaboration], *Elliptic flow of charged particles in Pb-Pb collisions at* $\sqrt{s_{NN}} = 2.76$ *TeV*, *Phys. Rev. Lett.* **105** (2010) 252302 [arXiv:1011.3914].

[11] G. Aad *et al.* [ATLAS Collaboration], *Measurement of the pseudorapidity and transverse momentum dependence of the elliptic flow of charged particles in lead-lead collisions at* $\sqrt{s_{NN}} = 2.76$ *TeV with the ATLAS detector*, *Phys. Lett.* **B707** (2012) 330 [arXiv:1108.6018].

[12] S. Chatrchyan *et al.* [CMS Collaboration], *Measurement of the elliptic anisotropy of charged particles produced in PbPb collisions at* $\sqrt{s}_{NN}$*=2.76 TeV*, *Phys. Rev.* **C87** (2013) 014902 [arXiv:1204.1409].

[13] T. Matsui and H. Satz, J/ψ *Suppression by Quark-Gluon Plasma Formation*, *Phys. Lett.* **B178** (1986) 416.

[14] N. Brambilla, A. Pineda, J. Soto, and A. Vairo, *Effective field theories for heavy quarkonium*, *Rev. Mod. Phys.* **77** (2005) 1423 [hep-ph/0410047].

[15] N. Brambilla, J. Ghiglieri, A. Vairo, and P. Petreczky, *Static quark-antiquark pairs at finite temperature*, *Phys. Rev.* **D78** (2008) 014017 [arXiv:0804.0993].

[16] L. D. McLerran and B. Svetitsky, *Quark Liberation at High Temperature: A Monte Carlo Study of SU(2) Gauge Theory*, *Phys. Rev.* **D24** (1981) 450.

[17] O. Kaczmarek, F. Karsch, P. Petreczky, and F. Zantow, *Heavy quark anti-quark free energy and the renormalized Polyakov loop*, *Phys. Lett.* **B543** (2002) 41 [hep-lat/0207002].

[18] P. Petreczky and K. Petrov, *Free energy of a static quark anti-quark pair and the renormalized Polyakov loop in three flavor QCD*, *Phys. Rev.* **D70** (2004) 054503 [hep-lat/0405009].

[19] O. Kaczmarek, F. Karsch, F. Zantow, and P. Petreczky, *Static quark anti-quark free energy and the running coupling at finite temperature*, *Phys. Rev.* **D70** (2004) 074505 [hep-lat/0406036].

[20] O. Kaczmarek and F. Zantow, *Static quark anti-quark interactions in zero and finite temperature QCD. I. Heavy quark free energies, running coupling and quarkonium binding*, *Phys. Rev.* **D71** (2005) 114510 [hep-lat/0503017].

[21] S.-J. Rey, S. Theisen, and J.-T. Yee, *Wilson-Polyakov loop at finite temperature in large-N gauge theory and anti-de Sitter supergravity*, *Nucl. Phys.* **B527** (1998) 171 [hep-th/9803135].

[22] A. Brandhuber, N. Itzhaki, J. Sonnenschein, and S. Yankielowicz, *Wilson loops in the large N limit at finite temperature*, *Phys. Lett.* **B434** (1998) 36 [hep-th/9803137].

[23] H. Boschi-Filho, N. R. Braga, and C. N. Ferreira, *Heavy quark potential at finite temperature from gauge/string duality*, *Phys. Rev.* **D74** (2006) 086001 [hep-th/0607038].

[24] O. Andreev and V. I. Zakharov, *On Heavy-Quark Free Energies, Entropies, Polyakov Loop, and AdS/QCD*, *JHEP* **04** (2007) 100 [hep-ph/0611304].

[25] S. I. Finazzo and J. Noronha, *Estimates for the Thermal Width of Heavy Quarkonia in Strongly Coupled Plasmas from Holography*, *JHEP* **11** (2013) 042 [arXiv:1306.2613].

[26] S. I. Finazzo and J. Noronha, *Debye screening mass near deconfinement from holography*, *Phys. Rev.* **D90** (2014) 115028 [arXiv:1411.4330].

[27] Y. Yang and P. H. Yuan, *Confinement-deconfinement phase transition for heavy quarks in a soft wall holographic QCD model*, *JHEP* **12** (2015) 161 [arXiv:1506.05930].

[28] D. Bak, A. Karch, and L. G. Yaffe, *Debye screening in strongly coupled $\mathcal{N} = 4$ supersymmetric Yang-Mills plasma*, *JHEP* **08** (2007) 049 [arXiv:0705.0994].

[29] A. Karch, E. Katz, D. T. Son, and M. A. Stephanov, *Linear confinement and AdS/QCD*, *Phys. Rev.* **D74** (2006) 015005 [hep-ph/0602229].

[30] O. Andreev and V. I. Zakharov, *The Spatial String Tension, Thermal Phase Transition, and AdS/QCD*, *Phys. Lett.* **B645** (2007) 437 [hep-ph/0607026].

[31] K. Kajantie, T. Tahkokallio, and J.-T. Yee, *Thermodynamics of AdS/QCD*, *JHEP* **01** (2007) 019 [hep-ph/0609254].

[32] S. S. Gubser and A. Nellore, *Mimicking the QCD equation of state with a dual black hole*, *Phys. Rev.* **D78** (2008) 086007 [arXiv:0804.0434].

[33] S. S. Gubser, A. Nellore, S. S. Pufu, and F. D. Rocha, *Thermodynamics and bulk viscosity of approximate black hole duals to finite temperature quantum chromodynamics*, *Phys. Rev. Lett.* **101** (2008) 131601 [arXiv:0804.1950].

[34] J. J. Friess, S. S. Gubser, G. Michalogiorgakis, and S. S. Pufu, *Stability of strings binding heavy-quark mesons*, *JHEP* **04** (2007) 079 [hep-th/0609137].

[35] T. Appelquist, M. Dine, and I. J. Muzinich, *The Static Potential in Quantum Chromodynamics*, *Phys. Lett.* **B69** (1977) 231.

[36] W. Fischler, *Quark-Antiquark Potential in QCD*, *Nucl. Phys.* **B129** (1977) 157.

[37] L. D. McLerran and B. Svetitsky, *A Monte Carlo study of SU(2) Yang-Mills theory at finite temperature*, *Phys. Lett.* **B98** (1981) 195.

[38] M. Laine, O. Philipsen, P. Romatschke, and M. Tassler, *Real-time static potential in hot QCD*, *JHEP* **03** (2007) 054 [hep-ph/0611300].

[39] A. Beraudo, J.-P. Blaizot, and C. Ratti, *Real and imaginary-time Q anti-Q correlators in a thermal medium*, *Nucl. Phys.* **A806** (2008) 312 [arXiv:0712.4394].

[40] Y. Burnier, O. Kaczmarek, and A. Rothkopf, *Static quark-antiquark potential in the quark-gluon plasma from lattice QCD*, *Phys. Rev. Lett.* **114** (2015) 082001 [arXiv:1410.2546].

[41] S.-J. Rey and J.-T. Yee, *Macroscopic strings as heavy quarks: Large-N gauge theory and anti-de Sitter supergravity*, *Eur. Phys. J.* **C22** (2001) 379 [hep-th/9803001].

[42] J. M. Maldacena, *Wilson loops in large N field theories*, *Phys. Rev. Lett.* **80** (1998) 4859 [hep-th/9803002].

[43] J. L. Albacete, Y. V. Kovchegov, and A. Taliotis, *Heavy Quark Potential at Finite Temperature in AdS/CFT Revisited*, *Phys. Rev.* **D78** (2008) 115007 [arXiv:0807.4747].

[44] Y. Kinar, E. Schreiber, and J. Sonnenschein, *Q anti-Q potential from strings in curved space-time: Classical results*, *Nucl. Phys.* **B566** (2000) 103 [hep-th/9811192].

[45] H. Liu, K. Rajagopal, and U. A. Wiedemann, *Wilson loops in heavy ion collisions and their calculation in AdS/CFT*, *JHEP* **03** (2007) 066 [hep-ph/0612168].

[46] H. Liu, K. Rajagopal, and Y. Shi, *Robustness and Infrared Sensitivity of Various Observables in the Application of AdS/CFT to Heavy Ion Collisions*, *JHEP* **08** (2008) 048, [arXiv:0803.3214].

[47] S. He, M. Huang, and Q.-S. Yan, *Logarithmic correction in the deformed* AdS_5 *model to produce the heavy quark potential and QCD beta function*, *Phys. Rev.* **D83** (2011) 045034 [arXiv:1004.1880].

[48] K. B. Fadafan, *Heavy quarks in the presence of higher derivative corrections from AdS/CFT*, *Eur. Phys. J.* **C71** (2011) 1799 [arXiv:1102.2289].

[49] C. Ewerz and K. Schade, *Applications of Holography to Strongly Coupled Plasmas*, *PoS* ConfinementX (2012) 270 [arXiv:1307.6161].

[50] D. Giataganas, *Probing strongly coupled anisotropic plasma*, *JHEP* **07** (2012) 031 [arXiv:1202.4436].

[51] A. Rebhan and D. Steineder, *Probing Two Holographic Models of Strongly Coupled Anisotropic Plasma*, *JHEP* **08** (2012) 020 [arXiv:1205.4684].

[52] E. Caceres, M. Natsuume, and T. Okamura, *Screening length in plasma winds*, *JHEP* **10** (2006) 011 [hep-th/0607233].

[53] A. Samberg and C. Ewerz, *Heavy Probes in Strongly Coupled Plasmas with Chemical Potential*, *Springer Proc. Phys.* **170** (2016) 401 [arXiv:1312.5999].

[54] S. D. Avramis, K. Sfetsos, and D. Zoakos, *On the velocity and chemical-potential dependence of the heavy-quark interaction in* $\mathcal{N} = 4$ *SYM plasmas*, *Phys. Rev.* **D75** (2007) 025009 [hep-th/0609079].

[55] O. Kaczmarek, *Screening at finite temperature and density*, *PoS* CPOD07 (2007) 043 [arXiv:0710.0498].

[56] M. Cheng *et al.*, *The QCD equation of state with almost physical quark masses*, *Phys. Rev.* **D77** (2008) 014511 [arXiv:0710.0354].

[57] S. Gupta, K. Hübner, and O. Kaczmarek, *Renormalized Polyakov loops in many representations*, *Phys. Rev.* **D77** (2008) 034503 [arXiv:0711.2251].

[58] K. Schade, *Applications of Holography to Strongly Coupled Plasmas*, PhD thesis, Universität Heidelberg, 2012.

[59] E. Nakano, S. Teraguchi, and W.-Y. Wen, *Drag force, jet quenching, and AdS/QCD*, *Phys. Rev.* **D75** (2007) 085016 [hep-ph/0608274].

[60] O. DeWolfe and C. Rosen, *Robustness of Sound Speed and Jet Quenching for Gauge/Gravity Models of Hot QCD*, *JHEP* **07** (2009) 022 [arXiv:0903.1458].

[61] O. Kaczmarek and F. Zantow, *Static quark anti-quark interactions at zero and finite temperature QCD. II. Quark anti-quark internal energy and entropy*, hep-lat/0506019.

[62] P. Petreczky, *Heavy quark potentials and quarkonia binding*, *Eur. Phys. J.* **C43** (2005) 51 [hep-lat/0502008].

[63] Y. Burnier, O. Kaczmarek, and A. Rothkopf, *Quarkonium at finite temperature: Towards realistic phenomenology from first principles*, *JHEP* **12** (2015) 101 [arXiv:1509.07366].

[64] I. Iatrakis and D. E. Kharzeev, *Holographic entropy and real-time dynamics of quarkonium dissociation in non-Abelian plasma*, *Phys. Rev.* **D93** (2016) 086009 [arXiv:1509.08286].

[65] K. B. Fadafan and S. K. Tabatabaei, *Entropic destruction of a moving heavy quarkonium*, arXiv:1512.08254.

[66] J. Noronha, *The Heavy Quark Free Energy in QCD and in Gauge Theories with Gravity Duals*, *Phys. Rev.* **D82** (2010) 065016 [arXiv:1003.0914].

[67] M. Abramowitz and I. A. Stegun, *Handbook of Mathematical Functions with Formulas, Graphs, and Mathematical Tables*, Dover Publications, 1964.

[68] M. Panero, *Thermodynamics of the QCD plasma and the large-N limit*, *Phys. Rev. Lett.* **103** (2009) 232001 [arXiv:0907.3719].

[69] U. Gürsoy, E. Kiritsis, L. Mazzanti, G. Michalogiorgakis, and F. Nitti, *Improved Holographic QCD*, *Lect. Notes Phys.* **828** (2011) 79 [arXiv:1006.5461].

[70] A. Bazavov *et al.*, *Equation of state and QCD transition at finite temperature*, *Phys. Rev.* **D80** (2009) 014504 [arXiv:0903.4379].

[71] S. S. Gubser, *Comparing the drag force on heavy quarks in N=4 super-Yang-Mills theory and QCD*, *Phys. Rev.* **D76** (2007) 126003 [hep-th/0611272].

[72] A. Bazavov and P. Petreczky, *Polyakov loop in 2+1 flavor QCD*, *Phys. Rev.* **D87** (2013) 094505 [arXiv:1301.3943].

[73] A. Bazavov, N. Brambilla, H.-T. Ding, P. Petreczky, H.-P. Schadler, A. Vairo, and J. H. Weber, *Polyakov loop in 2+1 flavor QCD from low to high temperatures*, [arXiv:1603.06637].

[74] D. E. Kharzeev, *Deconfinement as an entropic self-destruction: a solution for the quarkonium suppression puzzle?*, *Phys. Rev.* **D90** (2014) 074007 [arXiv:1409.2496].

[75] H. Satz, *Quarkonium Binding and Entropic Force*, *Eur. Phys. J.* **C75** (2015) 193 [arXiv:1501.03940].